An Experimental Study of the Influence of Elevated Buoyancy Levels on Flame Spread Rate Over Thermally Thin Cellulosic Materials

by
P. C. Shang
R. A. Altenkirch
and
R. Eichhorn

Department of
Mechanical Engineering

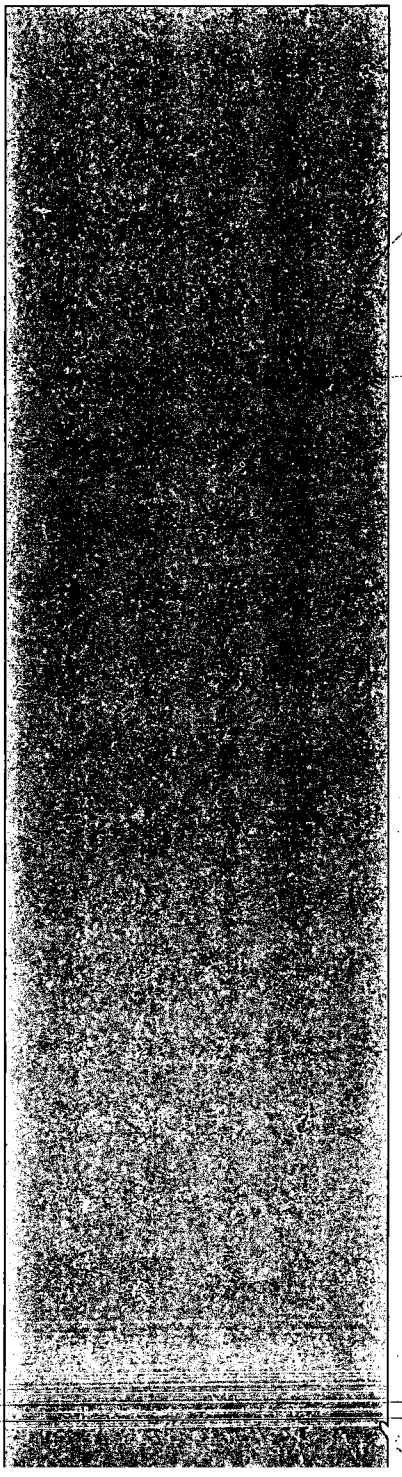

UKY-TR109-78-ME17
November 1978

A Report to the
National Aeronautics and
Space Administration

Supported by
Grant NSG-3114

College of Engineering
University of Kentucky
Lexington, Kentucky 40506

For additional copies or information
address correspondence to:
ORES Publications
College of Engineering
University of Kentucky
Lexington, KY 40506

A PUBLICATION OF THE OFFICE OF RESEARCH AND ENGINEERING SERVICES

UKY TR109-78-ME17
November 1978

An Experimental Study of the Influence of Elevated Buoyancy Levels on Flame Spread Rate Over Thermally Thin Cellulosic Materials

by

P.C. Shang
R.A. Altenkirch
and
R. Eichhorn
Department of Mechanical Engineering

A Report To The
National Aeronautics and Space Administration
Supported by
Grant NSG-3114

College of Engineering
University of Kentucky
Lexington, Kentucky

FOREWORD

Flame spread over solid combustible surfaces is a phenomenon of fundamental importance with a significant application to fire safety. From a practical point of view, it is important to be able to predict the flame spread rate over a variety of surfaces of arbitrary configuration and orientation and a range of environmental conditions. One of the aspects of flame propagation which is imperfectly understood is the role played by buoyancy in helping set the flame spread rate and its effect on extinction. There have been studies reported in which the buoyancy level has been varied by changing the ambient pressure and/or the inclination of the specimen. In one study, the results of experiments at nearly zero gravity level have been reported.

In work we report here, the buoyancy level has been changed by elevating the gravity level at which the experiments were conducted. The report describes the experimental setup and the results of a number of experiments conducted with it. For vertical downward flame spread over thermally thin paper samples, a dimensionless spread rate is found to correlate with a Damköhler number which varies with the ratio of the pressure to the gravity level. Different correlations are found for different ambient oxygen concentrations; for air the flames are extinguished when the Damköhler reaches a value of about 2×10^4. This corresponds to a pressure to gravity level of 2 kPa $\cdot s^2/m$.

A paper based on this work was presented at the Fall Meeting of the Western States Section/The Combustion Institute. It is referenced herein

as [21].

This report, except for a few pages replaced by this foreword, is identical to the senior authors' M.S.E. thesis in Mechanical Engineering. It represents an interim report on work sponsored under NASA-Lewis Grant NSG-3114 with T.H. Cochran as Project Monitor. Paul C. Shang is pleased to acknowledge partial support from an HEW Domestic Mining and Minerals Fellowship throughout the period of his studies and research. D.C. Winchester and P. Fluty were helpful collaborators in collecting the experimental data. Ms. Carol Marsh typed several versions of the report including the final copy.

TABLE OF CONTENTS

PAGE

APPENDIX

LIST OF FIGURES

CHAPTER I

INTRODUCTION

A. Brief Background on the Flame Spreading Problem

Flame spread over the surface of solid combustibles is of interest with respect to fire safety. Thus, a substantial amount of analytical and experimental work has been done in the past decade [1,2]*. However, due to the complexity of the flame spread phenomenon, complete understanding has not yet been achieved. The purpose of this investigation, which is mainly experimental in nature, is to provide information which will aid in the understanding of how buoyancy affects the flame spread phenomenon.

Figure 1 shows a schematic diagram of the problem associated with this work. A fuel bed is ignited at one edge, and following an initial transient period, a flame propagates steadily down the bed in a two dimensional fashion. Heat released by the flame and transferred forward of it vaporizes virgin fuel, producing the fuel vapor necessary to sustain the flame. In Fig. 1, a flow, which may be either naturally induced or forced, opposes the spreading flame.

The mechanism by which the flame in Fig. 1 propagates is by transferring heat to the unburnt fuel. For thin cellulosic specimens burnt

---

* Numbers in square brackets refer to literature citations in the Reference Section. Reviews by Sirignano [1] and Williams [2] give excellent discussions on the majority of those works. Only material pertinent to the present study will be discussed here.

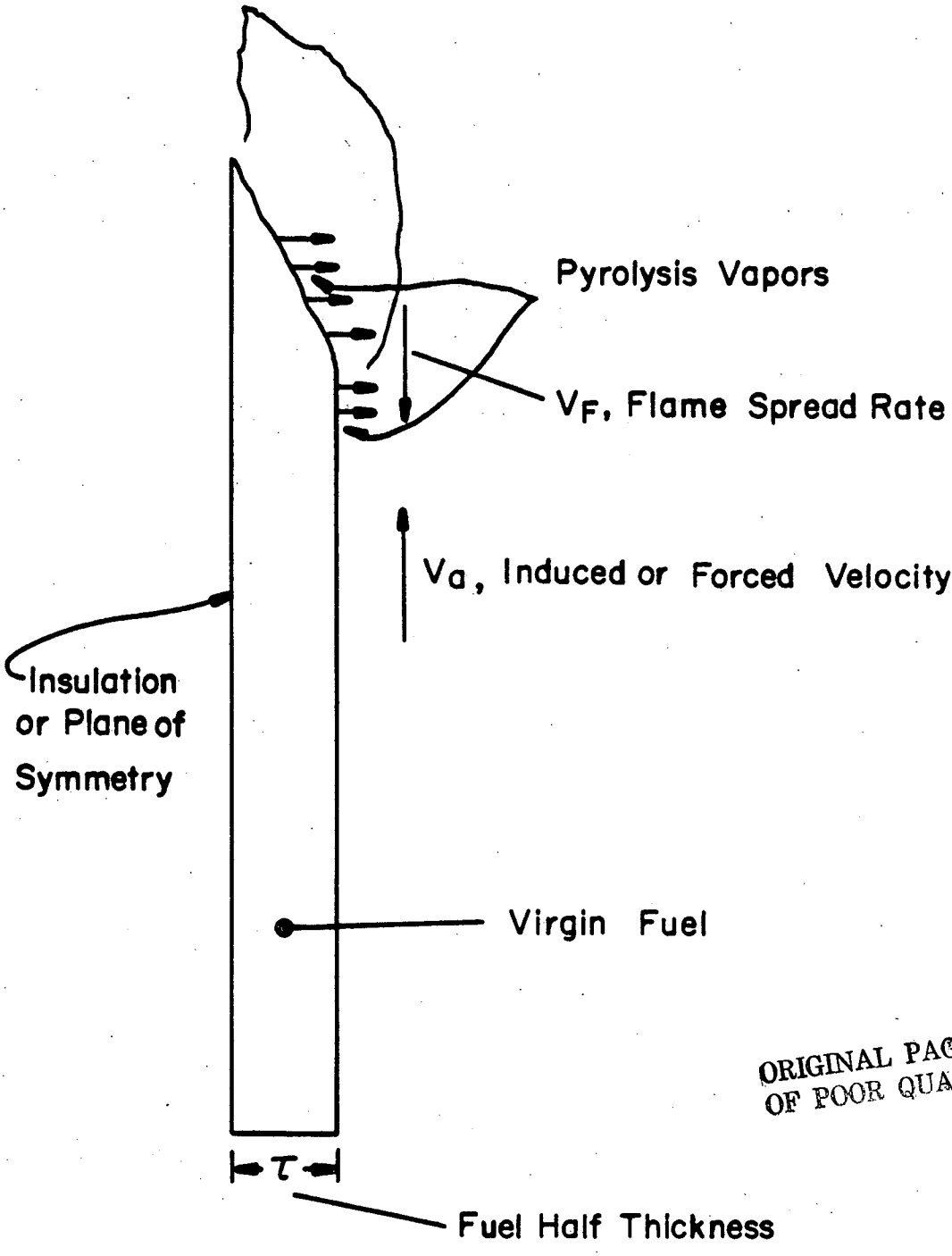

Figure 1. Flame spread process

vertically downward, heat transfer occurs by conduction in the gas phase [3]. Since no forward convective heat transfer is present, the opposing flow must be such that a local Peclet number is of order unity.

A fuel bed may not be heated appreciably prior to flame arrival. In this case, the bed is thermally thick. Lastrina et al. [4] characterized the fuel bed thickness by a dimensionless group,

$$\bar{\tau} = \frac{\tau}{\left(\frac{\alpha\delta}{V_F}\right)^{1/2}} \tag{1.1}$$

where τ is the dimensional bed half thickness, δ is the length ahead of the flame in which the temperature of the fuel bed surface rises from its initial temperature to a "burning" temperature, α is the thermal diffusivity of the fuel bed and V_F is the flame spread rate. A fuel bed is classified as thermally thick if $\bar{\tau} > 1$. Otherwise, the bed is thermally thin. Since the ignition length δ is dependent on the gas phase oxygen mole fraction and pressure, a particular fuel may be either thermally thick or thin depending on the environmental parameters. As a result, the usefulness of (1.1) is limited by the presence of this artificial ignition length.

Since pressure, fuel bed thickness, oxygen mole fraction and an opposing flow influence the flame spread rate, a great deal of attention has been given to the problem of determining the effects of these variables on the spread rate.

McAlevy and Magee [5] and Lastrina et al. [4] have found that flame spread rate data can be correlated with the empirical equation

$$V_F \propto (PY_{ox}^m)^{\Phi} \tag{1.2}$$

where P is the environment pressure, Y_{ox} is the environment oxygen mass fraction, and m and Φ are both dependent upon the type of specimen and diluent gas. For thermally thin cellulosic specimens burnt vertically downward, they reported a weak pressure dependence ($\Phi \simeq 0.1$) and a near unity mass fraction dependence ($m\Phi \simeq 1$).

Frey and T'ien [6] studied the effects of pressure, sample size and oxygen mole fraction using thermally thin paper samples. They observed that power law correlations such as (1.2) were inadequate for flames spreading near extinction.

The effects of an opposed flow on the flame spread rate for thin cellulosic specimens have been studied experimentally by Sibulkin et al. [7] and Hirano and Sato [8]. Sibulkin et al. obtained their data in a horizontal wind tunnel. Their results show that spread rate is nearly independent of free stream velocity, U_∞, for 15 cm/s $< U_\infty <$ 55 cm/s. As the free stream velocity is increased further, V_F gradually decreases until, for $U_\infty > 125$ cm/s, normal two dimensional burning no longer occurs. Data obtained by Hirano and Sato in a vertical wind tunnel show the same type of behavior.

The effects of buoyancy on flame spread over thin cellulosic speci-

mens have been studied by inclining the burning sample with respect to the vertical [7], thus generating a component of earth normal gravity along the direction of spread whose magnitude varies with inclination angle. However, one must interpret these data with caution as the usual fluid mechanical symmetry with respect to the specimen axis of symmetry is no longer present. It has been observed that at large angles to the vertical (usually > 30°) the flame on the underside of the specimen becomes unstable, and fluid flow there may be in the same direction as that of flame propagation [9, 10].

McAlevy and Magee [5] have shown that for thin cellulosic specimens, the vertical downward flame spread rate is inversely proportional to the specimen thickness. They obtained specimens of varying thickness by fusing wetted index cards together under high pressure. However, Fernandez-Pello and Williams [11] reported that two sheets of cellulosic material bonded together would spread apart under heating so that each sheet burnt independent of the other. They also reported that laminated sheets formed from more than two individual sheets or a single sheet placed against an insulating backing did not exhibit self sustained downward propagation.

Workers at NASA obtained spread rate data for thin cellulose acetate specimens burnt in zero and earth normal gravity environments [12, 13, 14]. In general, their results show that removal of buoyancy causes the spread rate to drop. However, since the usual product removal mechanism is absent in zero gravity flames, one must be careful in comparing zero and earth normal gravity data. The buildup of combustion products may partially quench the flame, causing it to propagate more slowly [15].

Some analytical work pertinent to the burning of thin cellulosic specimens is available. De Ris [16] assumed that the flame propagating over a fuel bed could be viewed as a thin diffusion flame. A uniform opposing flow was considered. Consequently, no forward convective heat transfer was allowed. By neglecting radiation effects and heat transfer in the fuel bed, the only forward heat transfer mechanism was gas phase conduction. A single global reaction was assumed to take place in the gas phase

$$\nu_f'(\text{Fuel}) + \nu_o' (\text{Oxygen}) \rightarrow \nu_p'' (\text{Product 1}) + \nu_p'' (\text{Product 2}) + \text{HEAT} \tag{1.3}$$

where ν is the stoichiometric coefficient and terms enclosed by parentheses are chemical formulas. Defining Schvab-Zeldovich variables, De Ris found the following expression for the flame spread rate:

$$V_F \tau \rho_s C_{ps} (T_{vap} - T_\infty) \simeq \sqrt{2}\, k (T_f - T_{vap}) \tag{1.4}$$

where

$$T_f = T_{vap} + (\underline{B} L/C_p)(1 - 1/K) - (T_{vap} - T_\infty) \tag{1.5}$$

$$K = [\underline{B}/\ln(1 + \underline{B})]^{-1}\, Q/(M_F \nu_f' L) \tag{1.6}$$

Here ρ_s is the fuel bed density, C_{ps} is the specific heat of the fuel bed, k is the gas phase thermal conductivity, T_{vap} is the fuel bed vaporization temperature, T_∞ is the environment temperature, T_f is the downstream asymptotic flame temperature, Q is the heat of combustion of $M_F \nu_f'$ grams of fuel, L is the latent heat of vaporization and $\underline{B}$ is the mass transfer

driving force. Note that in this expression V_F is independent of the opposing flow velocity. More recently, Frey and T'ien [17, 18] considered the same problem. In their formulation, the gas phase momentum equation was dispensed with through the use of the Oseen approximation. A one step second order reaction was assumed for gas phase oxidation, and a first order pyrolysis reaction was used for solid phase decomposition. Their numerical results show V_F to decrease continuously with an increasing uniform opposing flow, V_a. Although the solid and gas phase reaction rates and mechanisms are not known exactly, Frey and T'ien were able to predict flame extinction at low Damköhler numbers. The different dependence of V_F on the opposing flow velocity is because different chemical kinetics were used. De Ris assumed infinitely fast chemical kinetics; Frey and T'ien used finite rate chemical kinetics.

B. Objectives of Present Study

There is a substantial amount of literature on flame spread over thin solid combustibles. Most studies have shown experimental results and some correlations of the results. However, the effect of buoyancy has mostly been studied by inclining the fuel bed or by varying environmental pressure in the normal gravity environment of the earth. The only study in which the effects of buoyancy were investigated by varying gravity level has been the NASA zero gravity work.

The objectives of this investigation are to determine the effects of buoyancy on the flame spread rate over thin paper samples. Changes in pressure and gravity level affect the buoyant flow which is induced by

the hot downstream flame. The effects of these two parameters on the vertical downward flame spread rate over paper samples burnt in air and in a mixture which was 50% O_2/50% N_2 by volume were studied.

Previous correlations of flame spread results have been limited to some ad hoc empirical equations. It is also an objective of this study to correlate flame spread rates and independent physical parameters in dimensionless groups.

CHAPTER II

EXPERIMENT

A. Apparatus

A series of experimental studies of spread rate over paper samples of various sizes in various gas mixtures, at various pressures and gravity levels were undertaken to study the effects of buoyancy on flame spread. A test chamber and a centrifuge were needed to achieve the various environmental conditions required. They and other necessary apparatus for this experiment are described individually in the following sections.

1. The Test Chamber. The test chamber, shown in Fig. 2, was made of stainless steel and was designed in accordance with A.S.M.E. pressure vessel codes to withstand an internal pressure up to 3.4 MPa with a safety factor of four [19, 20]. The chamber consists of two 2:1 elliptical heads and a 32 cm diameter by 46 cm cylindrical main section. Chamber wall thickness is 0.5 cm. The overall length of the chamber is approximately 74 cm with an internal volume estimated at 0.037 m^3. Three transparent Plexiglas ports, 90 degrees apart with respect to each other, are located at the middle of the cylindrical section for viewing a specimen under test. A 10 x 15 cm elliptical opening,which can be closed by a 13 x 18 cm elliptical flange, is located at the bottom of the chamber for installing the test specimens.

Other features of the test chamber include:

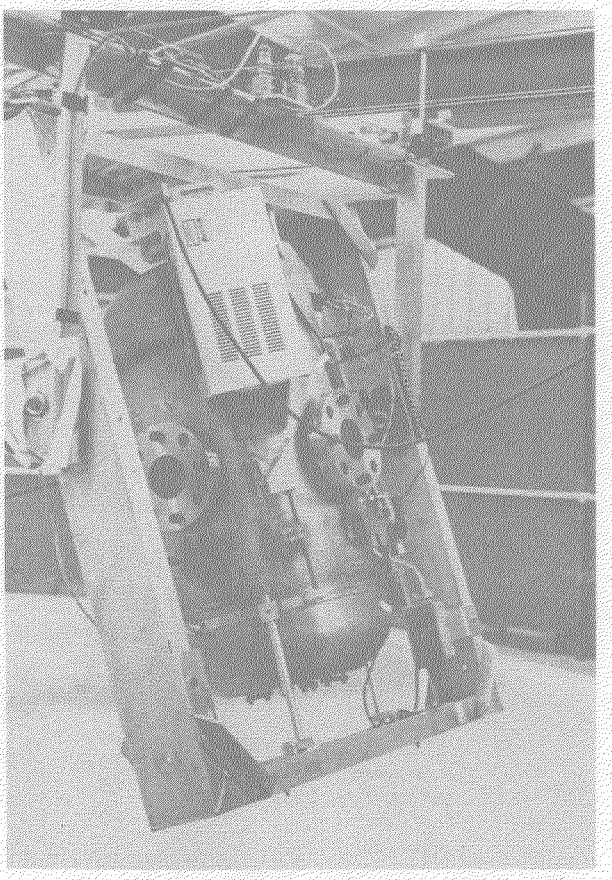

Figure 2. The test chamber showing a TV camera, mirror system and the supporting frame

(1) two electrical feedthroughs each rated at 2.8 MPa

(2) a rupture disc assembly (Fike) with a 2.2 MPa rated bursting pressure at 294 K

(3) a 3-way ball valve for isolating and venting the chamber

(4) a quick disconnect for connecting the test chamber to vacuum and gas supply systems (Fig. 3).

2. Centrifuge Facility. An existing 15 m diameter centrifuge, shown in Fig. 4, was used to create elevated gravity environments for studying flame spread. The centrifuge is located at the Wenner-Gren Aeronautical Research Laboratory, University of Kentucky. On each arm of the centrifuge is a carriage for mounting experimental packages. The radial position of the carriage as well as the centrifuge angular velocity are variable.

The centrifuge can offer a rotational speed as high as 186 s^{-1}, which, at a radius of 6.1 m, provides a gravity range up to 6.05 times earth normal gravity, g_e. However, at this radius, the strength of the centrifuge arms limits the range to 4.25 times earth normal gravity for a 55 kg package. To provide electrical requirements, the centrifuge has 24 sets of slip rings mounted on the drive shaft. Six sets were used for this experiment.

The centrifuge was designed to study the stress behavior of small animals under elevated gravity levels. A series of changes, adaptations, and apparatus designs were necessary to realize the objectives of this experiment. The following additions were made to the centrifuge: 1) a co-

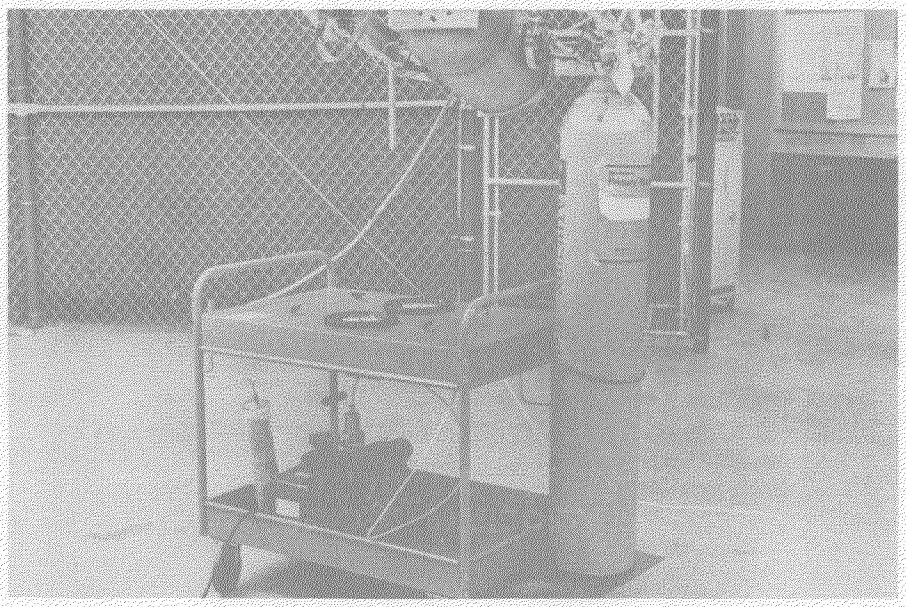

Figure 3. Instrumentation cart for establishing environmental conditions in the chamber

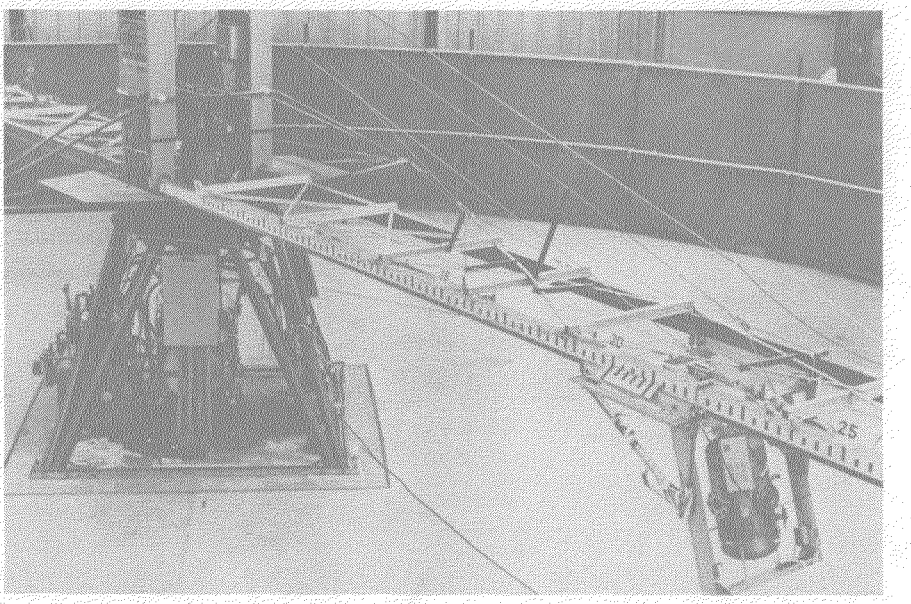

Figure 4. 15 m diameter centrifuge at the Wenner-Gren Aeronautical Research Laboratory

axial cable for transmitting television signals, 2) a closed circuit television system and a tape recorder, and 3) a remote ignition and time spread measurement system.

3. Specimen Holder and Spread Rate Measurement. The specimen holder used in this study consisted of two aluminum plates (0.079 cm thick). The holder, clamped together by four paper clips (Fig. 5), exposed a constant width, 1.92 cm, of sample for flame propagation. We wanted the sample width to be such that the spread rates were unaffected by the loss of thermal energy to the metal specimen holder. Therefore, tests were conducted at four sample widths with the results shown in Fig. 6. The 1.92 cm width was selected for the rest of the experiments as a minimum value for which only a slight width effect occurs.

For earth normal experiments, the flame was allowed to propagate a 3.8 cm distance before the start of spread time measurement so that the initial transient period was excluded. The spread time was then measured by a digital stop watch over a 5.08 cm fixed distance. The spread rates were slow enough (< 3 cm/s) to allow visual observations. The event that was actually timed was the movement of the dark pyrolysis front just behind the flame. This was easier to watch than the propagating flame.

Elevated gravity experiments required the ability to measure the spread time remotely and automatically. For this purpose, a mechanical device, consisting of cotton threads (shown as dotted lines in Fig. 5), microswitches and a clock was used to measure the time for the flame

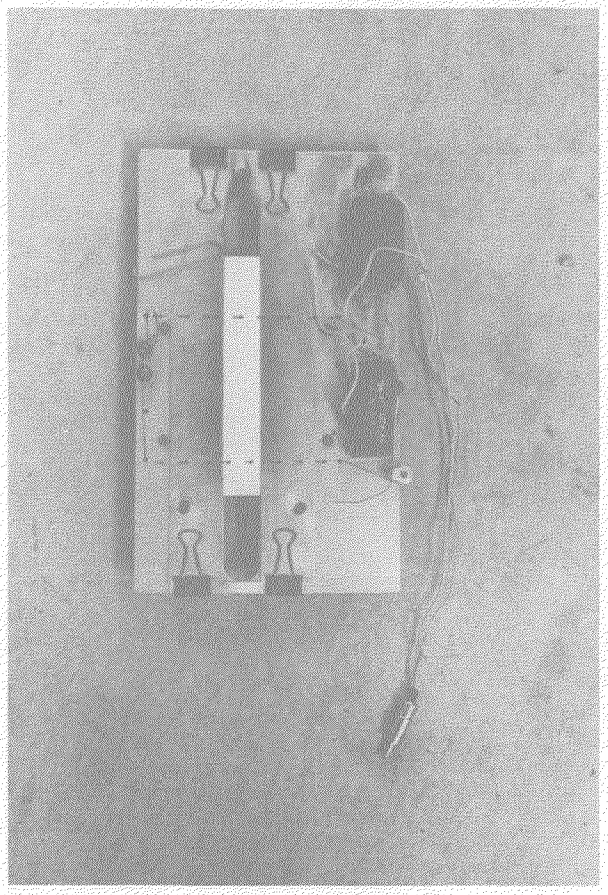

Figure 5. The specimen holder used for spread rate measurement. Dotted lines show the position of cotton threads on the backside.

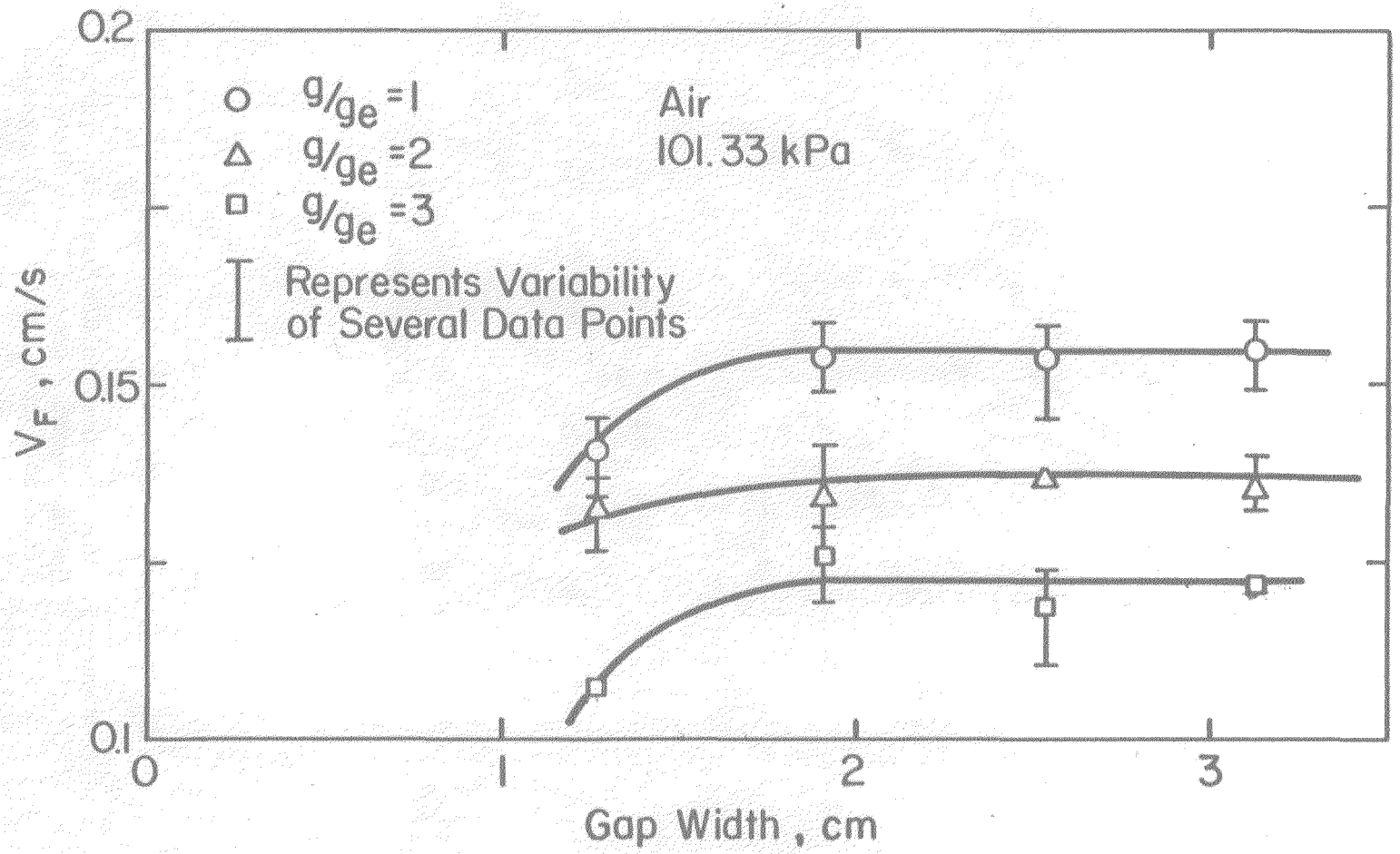

Figure 6. Dependence of V_F on the gap width allowed for flame propagation (index cards)

spread over a fixed distance (5.25 cm). Again, a 3.8 cm distance was allowed for the initial transient period. As the flame traverses the first cotton thread, a normally closed microswitch is tripped. This causes a relay to be energized which starts an electrical clock, graduated at 1/100 s. The breaking of the second thread trips a normally open microswitch, de-energizes the relay, and stops the clock. The difference in spread rates obtained by the two different methods is small and well within the probable experimental error.

4. The Mirror System. To provide for a permanent visual record of the spreading flames, a mirror system was developed so that a Bolex movie camera could be used to photograph both the edge and front views of the paper samples. When motion pictures were not desired, a television camera was mounted in place of the movie camera. In this way, the propagating flame could be observed when the centrifuge was rotating.

The mirror system, shown in Fig. 7, was devised to reflect the image of the flame to the level of the camera axis. The mirror outside each view port reflects the light emitted by the flame to the mirrors on the camera axis. These two mirrors then reflect front and edge views of the flame to the camera. By careful adjustment of the entire mirror system, the two views can be brought into focus simultaneously.

B. Procedure

Before an experiment, paper samples were dried for two hours in a Fisher vacuum oven at 373 K and 85 kPa. During this period, the oven

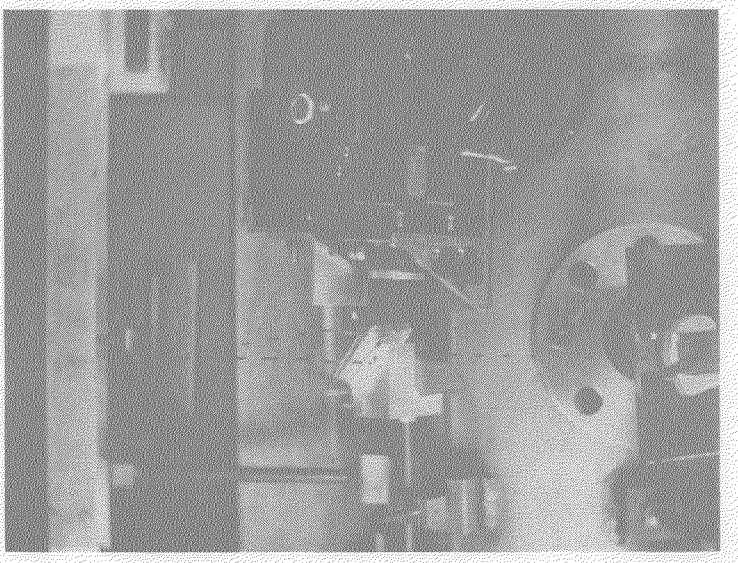

Figure 7. Configuration for taking pictures with a Bolex movie camera mounted on the chamber wall. Dotted lines represent light paths.

was constantly purged by dry nitrogen from a compressed gas bottle. After the paper samples were dried, they were placed in an air tight plastic jar containing a molecular sieve and tel-tale silica gel as a desiccant so that a relative humidity of nearly 0% could be maintained. These techniques are widely used to provide uniform samples and are necessary to achieve reproducible results.

The sample to be burnt was then placed between the two aluminum plates of the specimen holder. Three posts inside the chamber were used to mount the specimen holder, and its orientation was checked with a level prior to each run.

A nichrome wire (gage 29, 13 Ω/m) was used to ignite the paper sample. At elevated gravity, ignition of the paper sample using the igniter wire alone failed. Possibly, pyrolysis products were convected away by the buoyant flow induced by the igniter before ignition took place. In these instances a paper match was placed between the igniter and paper sample. The wire would first ignite the match head which would in turn ignite the sample.

To fill the test chamber to the desired pressure with a preselected gas mixture, the chamber was sealed, and vacuum and gas supply systems were connected. To insure that contamination was less than 1%, the test chamber was evacuated and purged before it was filled to the desired pressure. Chamber pressure was monitored by appropriate test gauges manufactured by Ametek. These pressure gauges were cleaned for oxygen service, and their accuracy was certified by the manufacturer to be

within 0.25% of full scale.

For earth normal gravity experiments, the spread rates were obtained by the technique described above. For elevated gravity experiments, additional preparation was required. The supporting frame was locked at an appropriate angle of tilt. This angle, which is a function of gravity level, was calculated so that the resultant of the earth normal gravity and the centrifugal acceleration was parallel to the surface of the paper sample for vertical downward flame spread. The actual tilt angle did not deviate from that calculated by more than 0.5 degrees.

Gravity levels were controlled by varying the rotational speed of the centrifuge at a fixed radius. A linear accelerometer (Schaevitz Model® LSB) whose output was amplified to give a 1 V/g_e reading on a digital voltmeter was mounted on the frame to indicate gravity level. The accelerometer was calibrated directly by rotating it, thus producing components of different magnitudes along its sensing axis. There is a maximum error of 0.3% in the accelerometer output. The accelerometer has a $\pm$ 25 g_e linear operating range. When the centrifuge had reached the desired rotational speed, the mechanical method described earlier was used to obtain the spread rate.

The air used in the experiments was supplied by a compressor. Moisture in the compressed air was removed by a heatless dryer. The 50% O_2/50% N_2 gas was supplied from a compressed gas cylinder whose contents were certified by Matheson Gas Products to be within 0.02% of the desired volume concentration.

CHAPTER III

RESULTS AND DISCUSSION

A. Results

During the earth normal gravity experiments, several motion pictures were taken. They cover a pressure range of 68.93 kPa up to 413.58 kPa for both index cards and paper tape burnt vertically downward in air. Motion pictures were also taken at varying gravity levels. Results of these motion pictures are discussed in the section on photographic observations.

About 90 vertical downward spread data for different gravities were recorded - - 58 in air, and 32 in the 50% O_2/50% N_2 mixture. These data are tabulated both in raw and dimensionless forms in Appendix C.

B. Power Law Correlation of Data

The pressure dependence of normal gravity spread rate data is usually correlated by power law relations [4, 5, 6]. Such results for vertical downward and horizontal spread from the present study are displayed in Figs. 8 through 11 to demonstrate that our measurement techniques are capable of reproducing results found in the literature. The straight lines shown in these figures are a calculated least square error fit to the data.

The pressure exponent of about 0.1 for vertical downward spread in air (Figs. 8 and 9) is typical of values found in the literature [5,6].

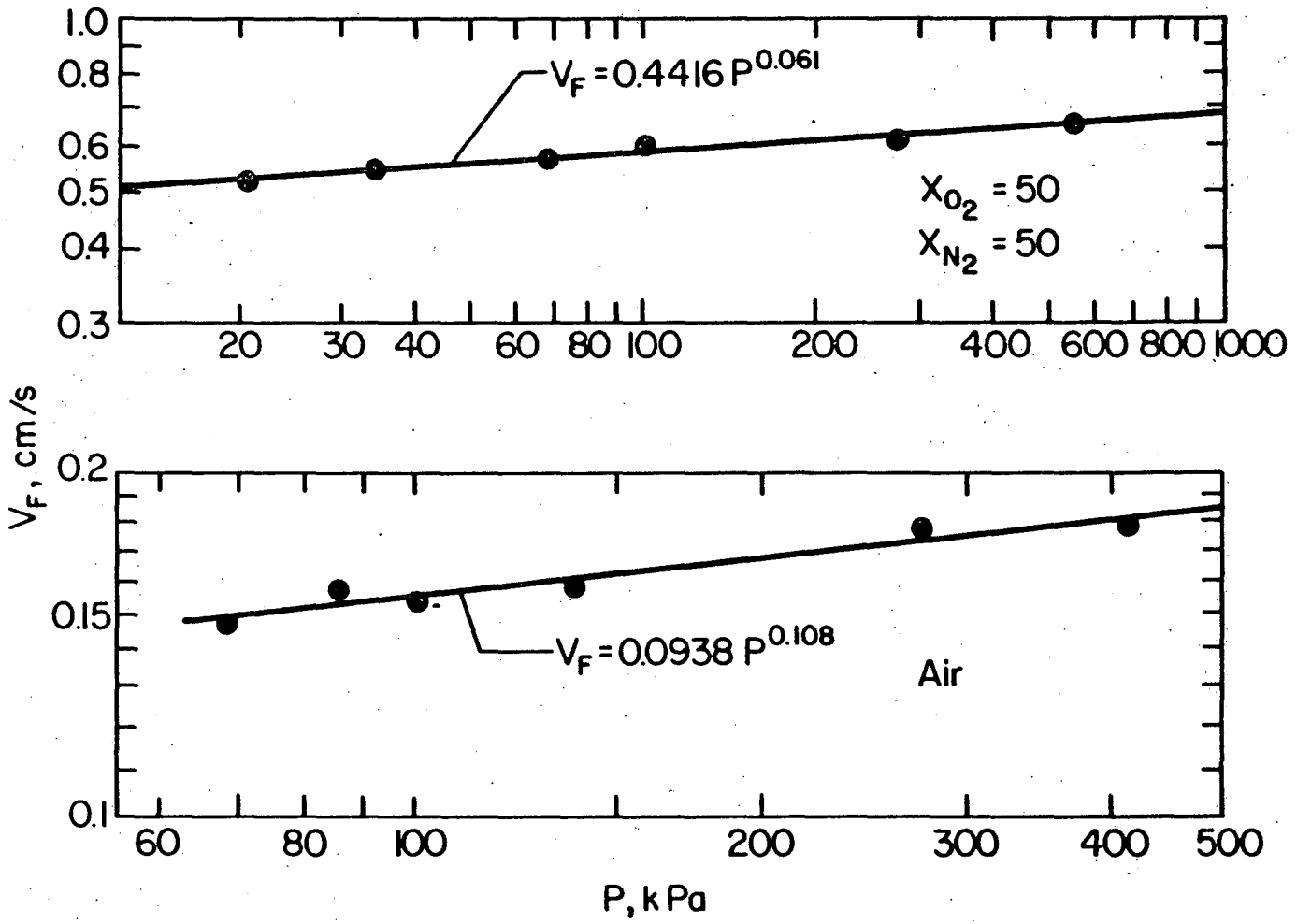

Figure 8. Pressure dependence of V_F for index cards (τ = 0.0098 cm) burnt vertically downward at normal gravity

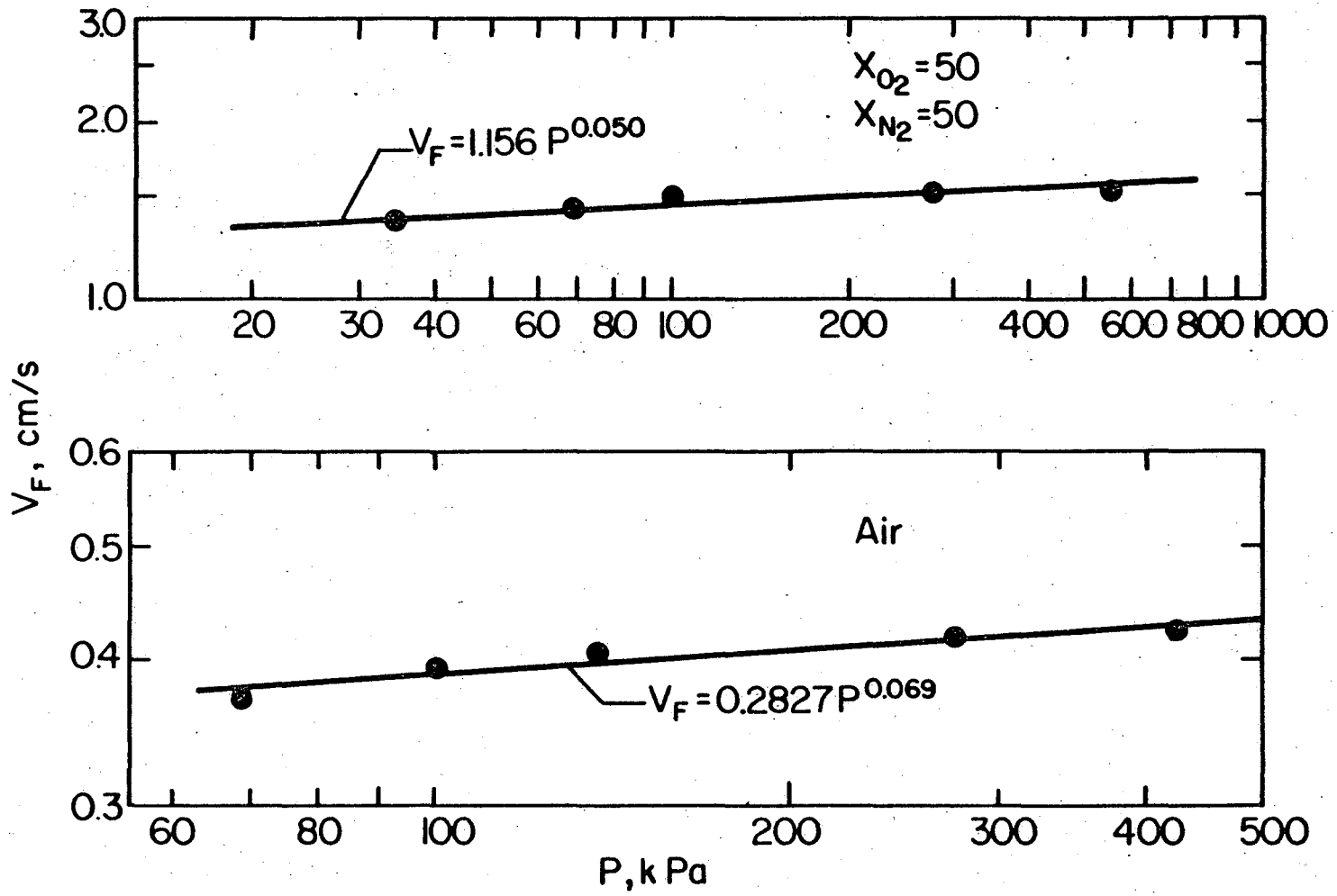

Figure 9. Pressure dependence of V_F for adding machine tape (τ = 0.0043 cm) burnt vertically downward at normal gravity

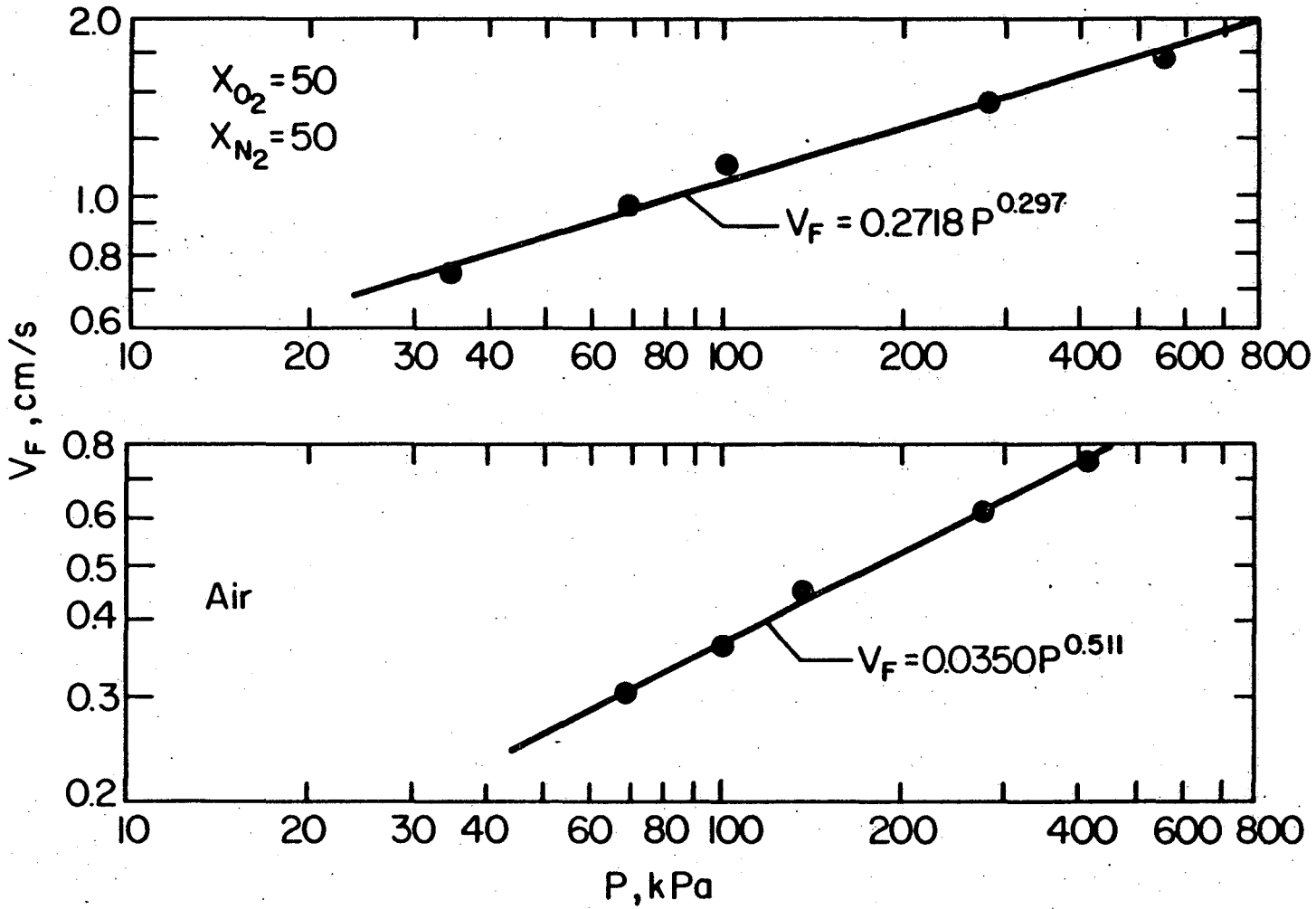

Figure 10. Pressure dependence of V_F for index cards (τ = 0.0098 cm) burnt horizontally at normal gravity

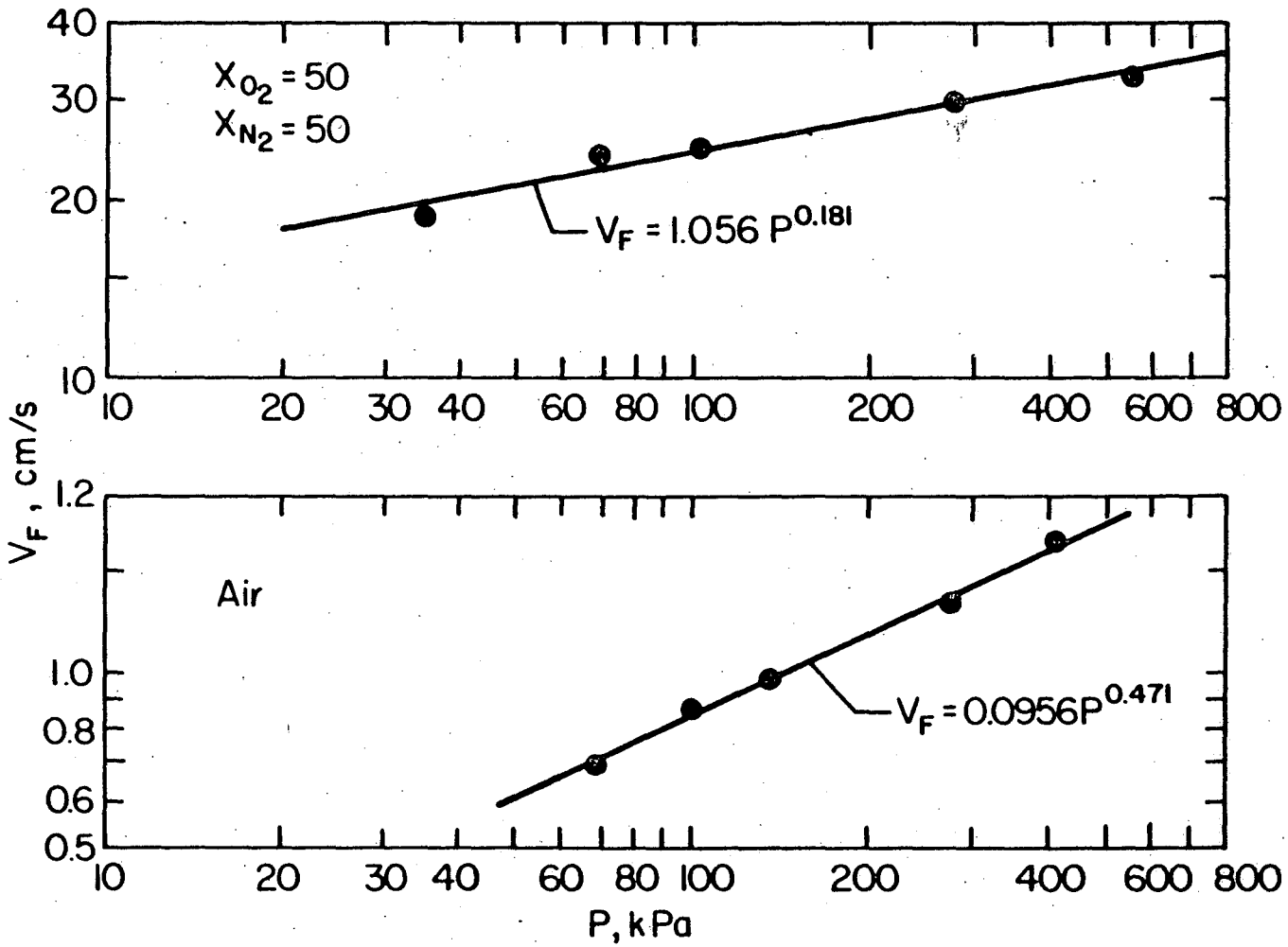

Figure 11. Pressure dependence of V_F for adding machine tape (τ = 0.0043 cm) burnt horizontally at normal gravity

The pressure dependence is smaller for the thinner specimens. The smaller pressure exponent for data obtained in a 50% O_2/50% N_2 mixture is probably because conditions are further from extinction as suggested by Frey and T'ien [6].

The pressure dependence for horizontal spread (Figs. 10 and 11) is dependent on the specimen thickness as well as the oxygen mole fraction. In general, the pressure exponent decreases with increasing oxygen mole fraction and decreasing specimen thickness for the same pressure range. Similar observations can be found in Ref. [6].

As noted previously, in the case of a paper sample, some investigators [9, 10] have observed unsteady fluid flow beneath the surface in the same direction as flame propagation, causing convective heat transfer ahead of the propagating flame. This results in a much faster spread rate and larger pyrolysis zone than for vertical downward flame spread. Hirano et al. [9] observed that this instability is dependent on the configuration and position of the remaining ash. Kashiwagi and Newman [10] reported that, for α - cellulose sheets (38 cm x 84 cm) shallow cuts normal to the direction of spread along the surface increased the frequency at which the ash shards fell. The unstable lower flame motion was then not observed. In the horizontal flame spread experiments done in our study, curling of the ash did not affect the flame, and the data were reproducible. The gap width allowed for flame propagation was 1.92 cm for all data reported. When the gap width was increased to 10 cm, a width comparable to that used by Hirano et al., curling of the ash started to affect the spread rate. For these wide samples, the remaining ash

divided into several portions with each portion assuming a different position. When a portion of the ash hung below the specimen surface, more fluid was forced toward the unburned material than when the ash was above the specimen surface. Also, the configuration of the remaining ash was time dependent. These two effects together give rise to erratic burning and an uneven pyrolysis front.

C. Dimensionless Correlation of Data

Correlations such as those displayed in Figs. 8 through 11 were obtained by varying one parameter while other parameters that may affect the spread rate were held constant. Such correlations are not particularly useful in attempting to determine the mechanism responsible for the behavior of the spreading flames. In this section, a method is presented of correlating in dimensionless form the physical parameters that affect flame spread.

In Figs. 12 through 14, dimensionless correlations of the vertical downward flame spread rate are displayed. The dimensionless groups used here to correlate spread rates appear as dimensionless parameters in the mathematical formulation of the vertical downward flame spread problem [21]. In each figure the abscissa is a Damköhler number; the ordinate is analogous to the fuel/air ratio in the region of flame attachment. The mass fraction of oxidizer also appears as a dimensionless parameter in the problem. Therefore, a different curve is generated for each mass fraction of oxygen. Values used for the various physical parameters are listed in Appendix C.

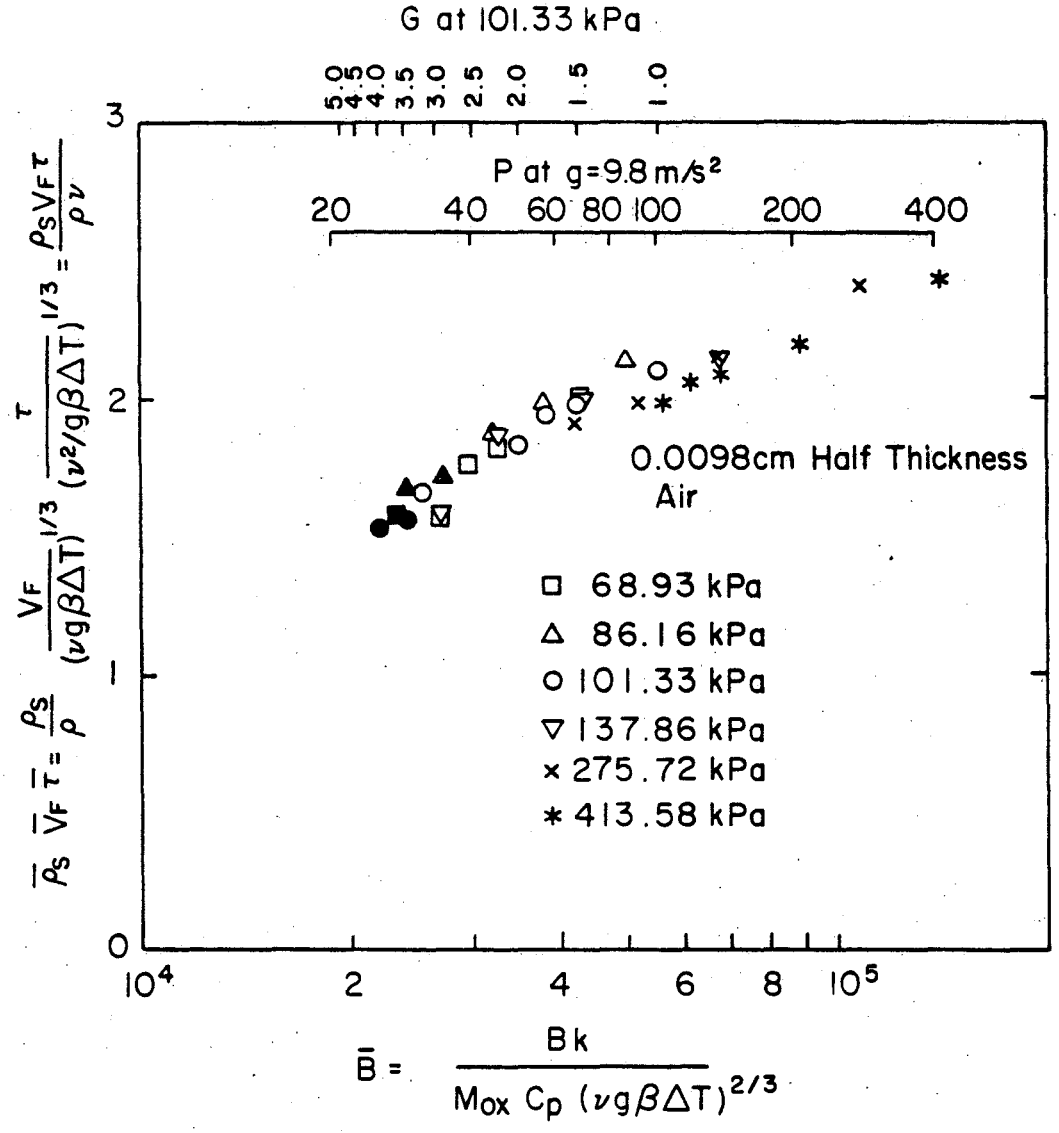

Figure 12. Dimensionless correlation of flame spread rate for index cards burnt vertically downward in air

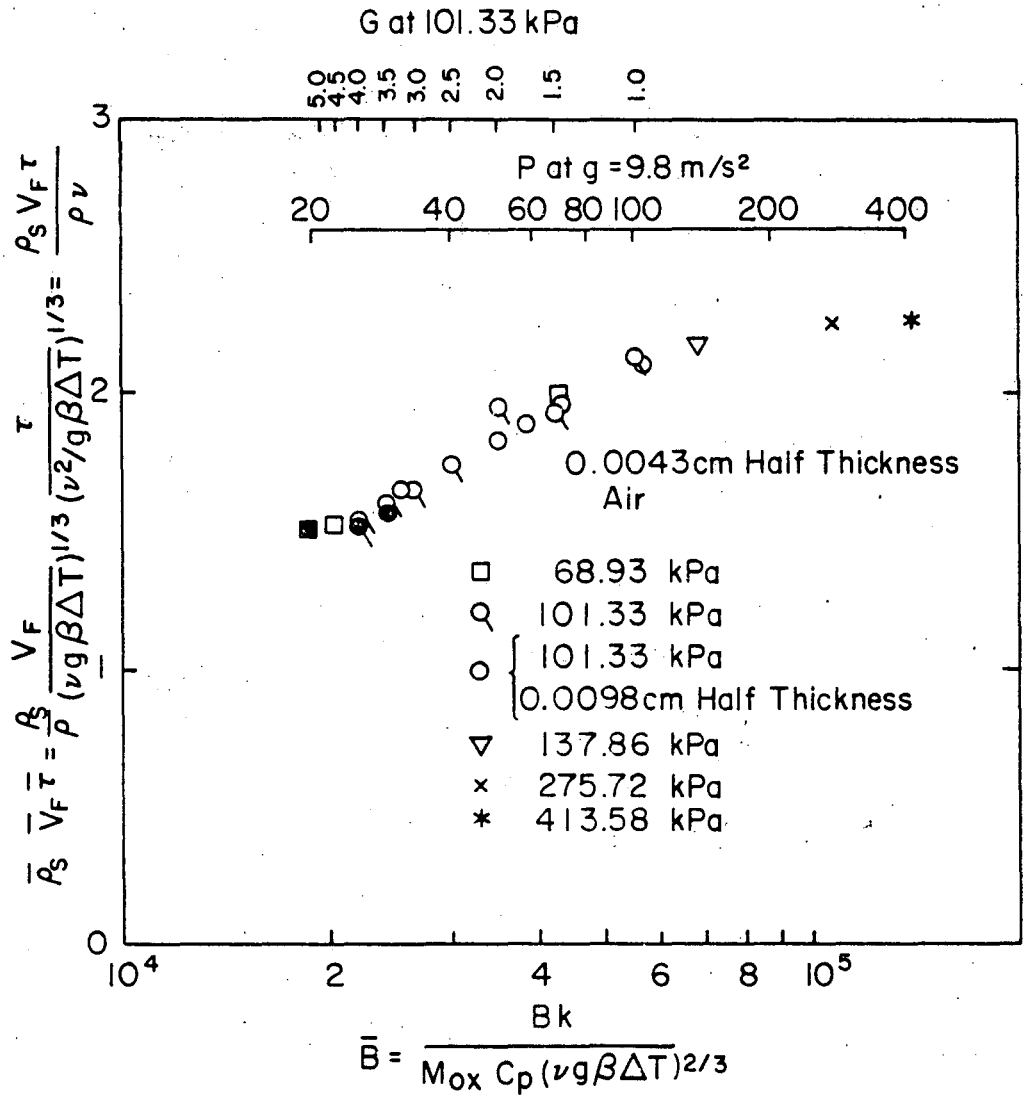

Figure 13. Dimensionless correlation of flame spread rate for adding machine tape burnt vertically downward in air

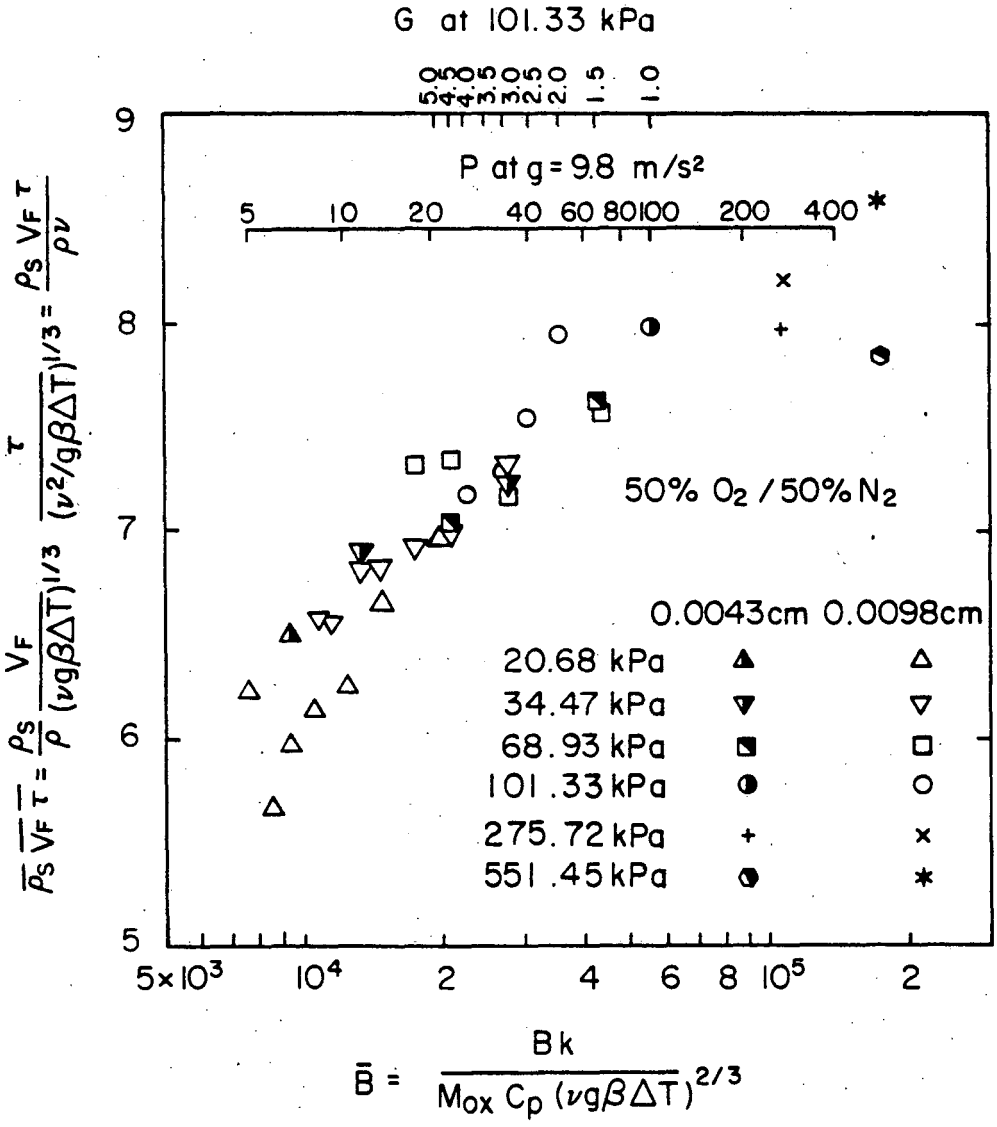

Figure 14. Dimensionless correlation of flame spread rate for index cards and adding machine tape burnt vertically downward in a 50% O_2/50% N_2 mixture

Frey and T'ien [18, 19] have used a similar correlation. In their theoretical analysis, they obtained a Damköhler number

$$\bar{B} = \frac{Bk}{C_p M_{ox} V_a^2} \tag{3.1}$$

as a dimensionless parameter in the energy equation. Here k and C_p are the gas phase thermal conductivity and specific heat at constant pressure, B is the gas phase pre-exponential factor of a presumed second order reaction and M_{ox} is the molecular weight of oxygen. A uniform flow velocity, V_a, opposing the flame, was implied through the use of an Oseen approximation. Their correlation was essentially a plot of V_F vs. $\bar{B}$ for a particular fuel thickness and density. The correlation presented here is dimensionless and includes these variations.

For the vertical downward flame spread case studied here, the fluid flow opposing the flame is a buoyant flow induced by the hot flame downstream of the point of flame attachment. The flow ahead of the flame must be sufficiently slow so that forward heat transfer by conduction through the gas phase is capable of sustaining propagation. Consequently, the usual boundary layer approximation for natural convection on a vertical flat plate is inapplicable. In the correlation presented here, the opposing flow velocity, V_a, is approximated by the characteristic buoyant velocity, $(\nu g \beta \Delta T)^{1/3}$. Here ν is the gas phase kinematic viscosity, g is the acceleration of gravity, β is the volumetric coefficient of expansion and ΔT is a characteristic temperature difference. This characteristic velocity is appropriate because in the vertical downward flame spread problem, as in the "general" vertical flat plate natural convection prob-

lem discussed by Hellums and Churchill [22], there is no real characteristic length. The Damköhler number defined in Eqn. 3.1 can therefore be written as

$$\overline{B} = \frac{Bk}{C_p M_{ox} (\nu g \beta \Delta T)^{2/3}} \tag{3.2}$$

The Damköhler number is the ratio of a fluid mechanical time, t_f, and the chemical time, t_c. For a unity Prandtl number, the Damköhler number becomes

$$\overline{B} = \frac{B\rho}{M_{ox}} \quad \frac{(\nu^2/g\beta\Delta T)^{1/3}}{(\nu g \beta \Delta T)^{1/3}} \tag{3.3}$$

Here $(B\rho/M_{ox})^{-1}$ is the chemical time. The ratio of $(\nu^2/g\beta\Delta T)^{1/3}$, the buoyant length, and $(\nu g \beta \Delta T)^{1/3}$, the buoyant velocity, represents the fluid mechanical time. The gas phase density is denoted by ρ.

As gravity increases or pressure decreases, the Damköhler number decreases. Since a decrease in Damköhler number means an increase in the chemical with respect to the fluid mechanical time, reactants have time to diffuse through the reaction zone, causing the flame temperature to drop. As a result, less heat is available for conduction heat transfer to the virgin fuel. Therefore, if the initial transient is excluded, there exists a Damköhler number below which a steadily propagating two dimensional flame is not possible. For index cards and paper tape burnt vertically downward in air, our results show that the flames are unable to spread below a Damköhler number of about 2.0×10^4. However, index

cards and paper tape extinguish at slightly different Damköhler numbers. Possibly, this result can be an effect of slight differences in chemical composition which would cause different gas phase pre-exponential factors for the two cases. The same pre-exponential factor was used in correlating the data. Figures 12 and 13 display such results. As the extinction limit was approached, one or more of the attempts to obtain a steadily propagating flame would fail. For those values of $\bar{B}$, the results are shown as filled data points.

The ordinate, $\bar{\rho}_s \bar{V}_F \bar{\tau}$, is

$$\bar{\rho}_s \bar{V}_F \bar{\tau} = \frac{\rho_s}{\rho} \frac{V_F}{(\nu g \beta \Delta T)^{1/3}} \frac{\tau}{(\nu^2/g\beta\Delta T)^{1/3}} \qquad (3.4)$$

or

$$\bar{\rho}_s \bar{V}_F \bar{\tau} = \frac{\rho_s V_F \tau}{\mu} \qquad (3.4a)$$

where $\rho_s \tau$ is the paper sample area density and μ is the dynamic viscosity. The numerator, $\rho_s V_F \tau$, is proportional to the amount of fuel available for combustion per unit sample width. The denominator, μ, is proportional to the mass flux of gas mixture per unit sample width. Note that $\bar{\rho}_s \bar{V}_F \bar{\tau}$ is independent of pressure and gravity level. Therefore, the characteristic mass flux of gas mixture per unit width is independent of pressure and gravity level. It would be interesting to know whether or not the actual mass flux per unit sample width is also independent of pressure and gravity level. However, this would require complete knowledge of the gas phase velocity and temperature profiles.

As we showed in Fig. 6, for gap widths $\geq$ 1.92 cm, the flame spread rate for vertical downward flame spread in air up to three times earth normal gravity is unaffected by specimen width when the sample is clamped in aluminum plates. Also, Frey and T'ien [6] found the influence of gap width decreased as oxygen mole fraction was increased. The experimental results obtained here show that the numerical predictions of Frey and T'ien [18, 19], which have V_F continuously decreasing as $\overline{B}$ decreases, are qualitatively correct.

$\overline{\rho}_s \overline{V}_F \overline{\tau}$ as a function of $\overline{B}$ has a continuously decreasing slope with increasing $\overline{B}$. As $\overline{B} \to \infty$, the parameter $\overline{\rho}_s \overline{V}_F \overline{\tau}$ may become independent of $\overline{B}$ and possibly approach the thin flame limit of De Ris [16].

$$\overline{\rho}_s \overline{V}_F \overline{\tau} = \frac{\sqrt{2} C_p}{C_{ps}} \frac{T_f - T_{vap}}{T_{vap} - T_\infty} \tag{3.5}$$

Using values of T_{vap} and C_{ps} from Frey and T'ien [18] and De Ris' downstream asymptotic flame temperature, we found a value of 5.9 for air. Figures 12 and 13 show that $\overline{\rho}_s \overline{V}_F \overline{\tau}$, as a function of $\overline{B}$, appears to approach an asymptotic value. If $\overline{B}$ is increased further, we expect the spread rate to become independent of the opposing buoyant flow.

Portions of the present correlation for air that are away from the extinction limit ($\overline{B} > 4 \times 10^4$) exhibit $V_F \propto g^{-1/9}$, or $V_F \propto V_a^{-1/3}$. Data from Sibulkin et al. [7] and Hirano and Sato [8] show this type of dependence in certain ranges of V_a (Figs. 15 and 16). In these wind tunnel experi-

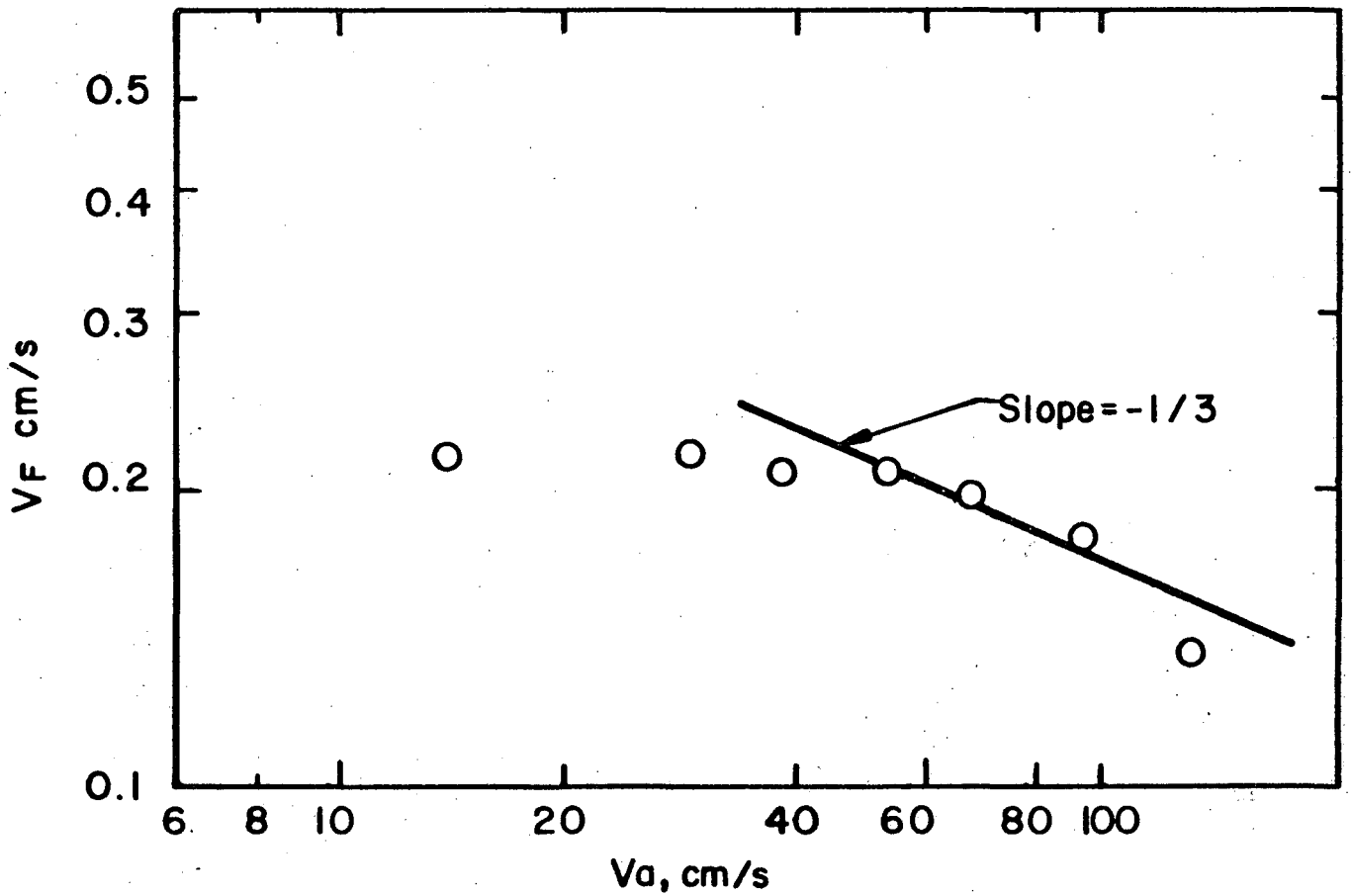

Figure 15. Dependence of V_F on the forced velocity V_a. Data taken from Ref. [7].

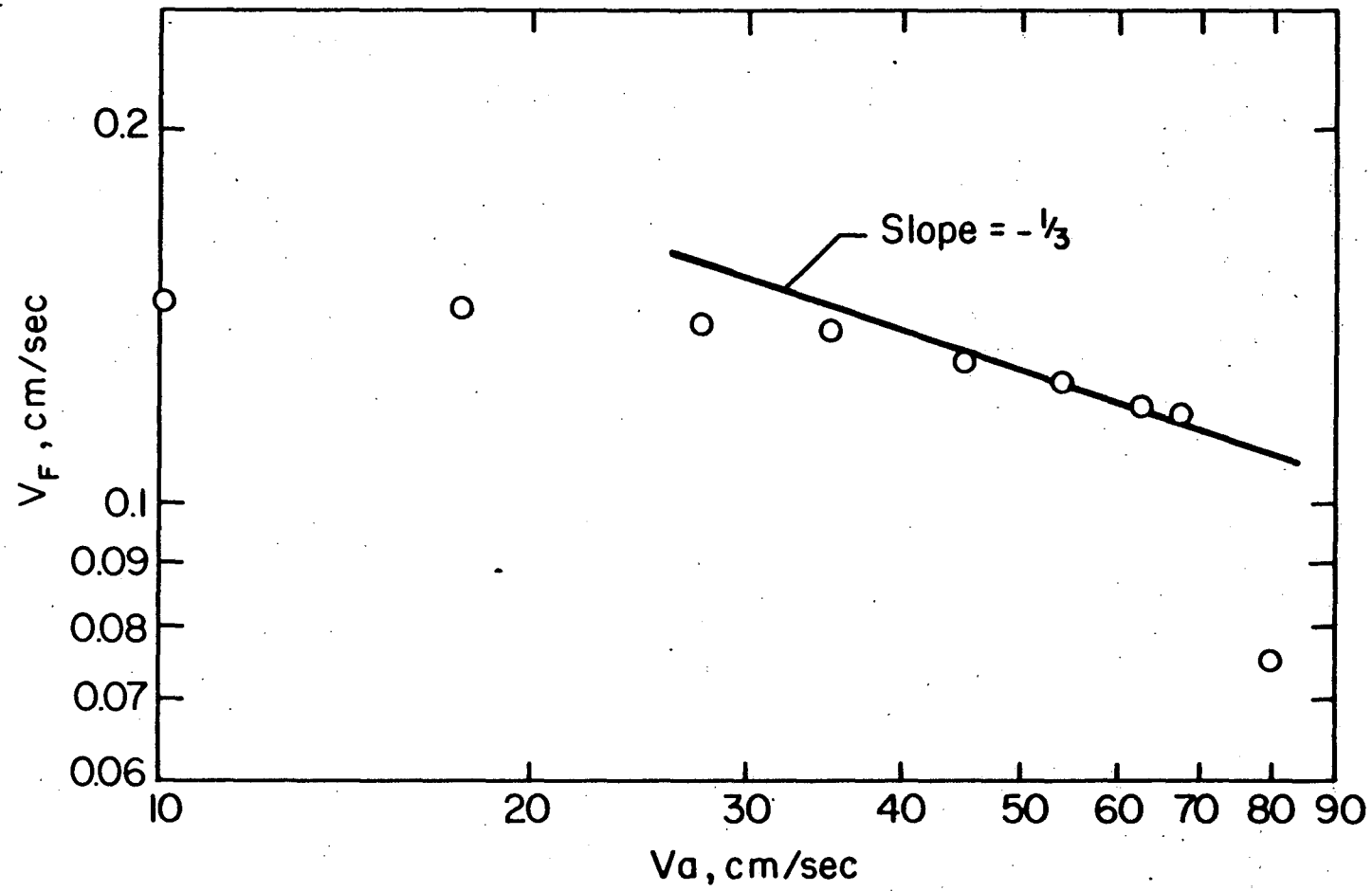

Figure 16. Dependence of V_F on the forced velocity V_a. Data taken from Ref. [8].

ments, a laminar boundary layer whose thickness varies as $U_\infty^{-1/2}$ was always present. From the data of Hirano and Sato [8], the boundary layer thickness appears to be substantially greater than the downstream flame stand-off distance. Consequently, for the lower velocity points, the flame would be expected to be entirely immersed in the slow flow region next to the surface. This observation may explain the independence of the flame spread rate on flow velocity for the lower free stream velocities in these experiments. The boundary layer thickness was calculated based on the sample length of Hirano and Sato.

The $V_F \propto V_a^{-1/3}$ relationship for the air results implies that, at a constant gravity level, the flame spread rate is proportional to $P^{1/9}$. Such dependence is consistent with the pressure exponent of about 0.1 reported by McAlevy and Magee [5] and with the data shown in Fig. 8. Also, $V_F \propto g^{-1/9}$ is implied by $V_F \propto V_a^{-1/3}$. The inclined bed data of Sibulkin et al. [7] exhibit this type of dependence at angles near vertical (Fig. 17).

D. Photographic Observations

1. Normal Gravity Photographs. Motion pictures of vertical downward flame spread on index cards and paper tape were taken at several pressures. From these motion pictures, we saw that the flame color was greatly dependent on the pressure level. At high pressure (i.e. high Damköhler number) luminous flames occurred whose color was orange with a small bluish region near the area of flame attachment. The flame size was smaller than those at a lower pressure, indicating that the chemical

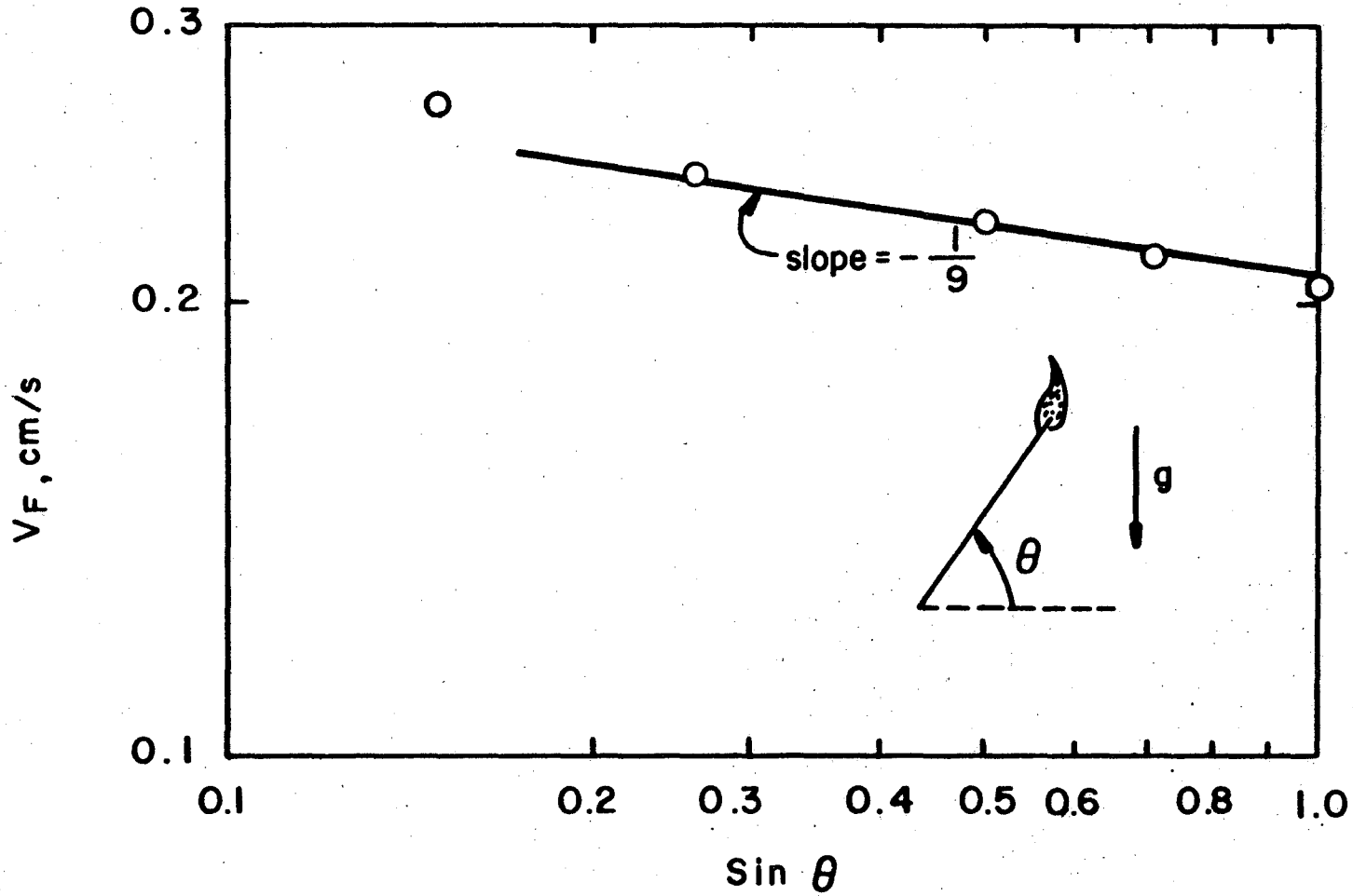

Figure 17. Dependence of V_F on the orientation for thin paper samples. Data taken from Ref. [7].

reactions were fast and only occurred in a small region. As the pressure was reduced, the residence time of the reactants in the flame zone was increased. The flame gradually transformed into a blue colored flame with a visible orange glowing char. This decrease in luminosity was caused by a local decrease in fuel/air ratio. Flame size was greatly enlarged at lower pressures. The flame shape in all cases was boundary layer like.

2. Photographs with Identical Damköhler Number. Motion pictures of vertical downward flame spread on index cards were taken at $\overline{B} \simeq 14 \times 10^4$ and $\overline{B} \simeq 2.7 \times 10^4$ in an attempt to verify the present model. $\overline{B} \simeq 14 \times 10^4$ was obtained at 413.58 kPa and $4g_e$, and at 101.33 kPa and $1g_e$. $\overline{B} \simeq 2.7 \times 10^4$ was obtained at 68.93 kPa and $2g_e$, and at 137.86 kPa and $4g_e$.

These pictures revealed that flames with identical Damköhler number did not have the same characteristics. Instead, flame size and color seemed to be unaffected by changes in gravity level. This suggests that for flames of identical Damköhler number, only regions near the flame attachment area are identical. However, in our experiments, this region could not be photographed as the aluminum plates' thickness is about the same as the flame stand-off distance near the foot of flame attachment [9].

CHAPTER IV

CONCLUSIONS

The dependence of flame spread on buoyancy has been demonstrated by varying gravity level and pressure. The flame spread rate is shown to decrease as the buoyancy induced flow increases.

A method of correlating flame spread data using dimensionless parameters has been presented. Flame spread rate, V_F, is expressed by

$$\overline{\rho_s} \overline{V_F} \overline{\tau} = \frac{\rho_s V_F \tau}{\mu} \qquad (4.1)$$

which allows variations in sample thickness and density. The Damköhler number

$$\overline{B} = \frac{Bk}{C_p M_{ox} (\nu g \beta \Delta T)^{2/3}} \qquad (4.2)$$

is the dependent variable. If the Damköhler number is reduced, the flame spread rate drops until extinction occurs. The extinction limit is about $\overline{B} = 2.0 \times 10^4$ for paper samples burnt in air.

REFERENCES

1. Sirignano, W.A., A Critical Discussion of Theories of Flame Spread Across Solid and Liquid Fuels, Combustion Science and Technology, 6, 95-105, 1972.

2. Williams, F.A., Mechanisms of Fire Spread, Sixteenth Symposium (International) on Combustion, The Combustion Institute, Pittsburgh, PA, 1281-1294, 1977.

3. Parker, W.J., Flame Spread Model for Cellulosic Materials, Journal of Fire and Flammability, 3, 254-269, 1972.

4. Lastrina, F.A., Magee, R.S. and McAlevy, R.F. III, Flame Spread Over Fuel Beds: Solid-Phase Energy Considerations, Thirteenth Symposium (International) on Combustion, The Combustion Institute, Pittsburgh, PA , 935-948, 1971.

5. McAlevy, R.F. III and Magee, R.S., The Mechanism of Flame Spreading Over the Surface of Igniting Condensed-Phase Materials, Twelfth Symposium (International) on Combustion, The Combustion Institute, Pittsburgh, PA , 215-227, 1969.

6. Frey, A.E. Jr. and T'ien, J.S., Near-Limit Flame Spread and Flame Structure for Thermally Thin Paper Samples, Report FTAS/TR-75-116, Case Western Reserve University, 1975.

7. Sibulkin, M., Ketelhut, W. and Feldman, S., Effect of Orientation and External Flow Velocity on Flame Spreading over Thermally Thin Paper Strips, Combustion Science and Technology, 9, 75-77, 1974.

8. Hirano, T. and Sato, K., Effects of Radiation and Convection on Gas Velocity and Temperature Profiles of Flame Spreading Over Paper, Fifteenth Symposium (International) on Combustion, The Combustion Institute, Pittsburgh, PA , 233-241, 1975.

9. Hirano, T., Noreikis, S.E. and Waterman, T.E., Measured Velocity and Temperature Profiles of Flames Spreading Over a Thin Combustible Solid, IIT Research Institute, Interim Technical Report No. 2, Project J-1139, 1973.

10. Kashiwagi, T. and Newman, D.L., Flame Spread Over an Inclined Thin Fuel Surface, Combustion and Flame, 26, 163-177, 1976.

11. Fernandez-Pello, A. and Williams, F.A., Experimental Techniques in the Study of Laminar Flame Spread over Solid Combustibles, Combustion Science and Technology, 14, 155-167, 1976.

12. Andracchio, C.R. and Aydelott, J.C., Comparison of Flame Spreading Over Thin Flat Surfaces in Normal Gravity and Weightlessness in an Oxygen Environment, NASA TM X-1992, 1972.

13. Andracchio, C.R. and Cochran, T.H., Burning of Solids in Oxygen-Rich Environments in Normal and Reduced Gravity, NASA TM X-3055, 1974.

14. Andracchio, C.R. and Cochran, T.H., Gravity Effects on Flame Spreading Over Solid Surfaces, NASA TN D-8828, 1976.

15. Altenkirch, R.A., Eichhorn, R., Hsu, N.N., Brancic, A.B. and Cevallos, N.E., Characteristics of Laminar Gas Jet Diffusion Flames Under the Influence of Elevated Gravity, Sixteenth Symposium (International) on Combustion, The Combustion Institute, Pittsburgh, PA , 1165-1174, 1977.

16. De Ris, J.N., Spread of a Laminar Diffusion Flame, Twelfth Symposium (International) on Combustion, The Combustion Institute, Pittsburgh, PA , 241-252, 1969.

17. Frey, A.E. Jr. and T'ien, J.S., A Theory of Flame Spread Over a Solid Fuel Including Finite Rate Chemical Kinetics, Central States Section/The Combustion Institute Spring Meeting, 1977.

18. Frey, A.E. Jr. and T'ien, J.S., A Theory of Flame Spread Over a Solid Fuel Including Finite Rate Chemical Kinetics, Report FTAS/TR-77-134, Case Western Reserve University, 1977.

19. Megresy, E.F., Pressure Vessel Handbook, Pressure Vessel Handbook Publishing, Inc., Tulsa, OK, 1973.

20. Roark, R.J., Formulas for Stress and Strain, Fourth Edition, McGraw-Hill Book Company, New York, 1965.

21. Altenkirch, R.A., Shang, P.C. and Eichhorn, R., An Experimental Study of the Effects of Buoyancy on Flames Spreading Down Thermally Thin Paper Samples, Western States Section/ The Combustion Institute Fall Meeting, 1978.

22. Hellums, J.D. and Churchill, S.W., Dimensional Analysis and Natural Circulation, Chemical Engineering Progress Symposium Series, 57, 75-80, 1961.

23. Sun, K. and Lienhard, J.H., The Peak Pool Boiling Heat Flux on Horizontal Cylinders, College of Engineering Bulletin No. 88, University of Kentucky, 1969.

24. Eckert, E.R.G. and Drake, R.M. Jr., Analysis of Heat and Mass Transfer, McGraw-Hill Book Company, New York, 1972.

25. CRC Handbook of Chemistry and Physics, 55th Edition, CRC Press, Inc., Cleveland, OH, 1975.

26. JANAF Thermochemical Tables, Second Edition, National Bureau of Standards, 1971.

27. Reid, R.C., Prausnitz, J.M. and Sherwood, T.K., The Properties of Gases and Liquids, Third Edition, McGraw-Hill Book Company, New York, 1977.

APPENDIX A

ERROR IN EXPERIMENTS

1. Oxygen Mole Fraction Changes During a Run

The most severe changes in oxygen mole fraction inside the chamber occur during the burning of index cards in the 50% O_2/50% N_2 mixture at 20.68 kPa. For reasons explained in the Spread Rate Measurement section, a 7.52 cm by 1.92 cm strip of index card is considered here for analysis purposes.

Such a paper sample has a mass of 0.21 g (Appendix C). Assuming pure cellulose, $(C_6H_{10}O_5)_x$, we use the following reaction to estimate the oxygen mole fraction changes:

$$C_6H_{10}O_5 + 6O_2 \rightarrow 6CO_2 + 5H_2O$$

The molecular weight of the cellulose monomer is 162 g/mol. Therefore, 1.30×10^{-3} moles of cellulose and 7.82×10^{-3} moles of oxygen were consumed during each experiment. At standard conditions, the test chamber contains 0.346 moles of gas. Hence, for a 50% O_2/50% N_2 gas mixture at 20.68 kPa, there are 0.173 moles of oxygen available for combustion. It follows that the total percentage change in the oxygen mole fraction is no more than 0.8%.

2. Error Analysis

The error in determining the flame spread rate, V_F, is the error

in spread rate measurement which includes two variables, t and d. The relation between these two variables can be written in the following form

$$V_F = \frac{d}{t} \tag{A-1}$$

where d and t are the distance and the time for the flame to travel the distance. Therefore, the error of V_F by measurement is the combination of the errors caused by measuring d and t.

The variation of V_F by measurement can be analyzed by the standard error analysis method [23]. Equation A-1 is differentiated and divided by V_F. Therefore,

$$\frac{\Delta V_F}{V_F} = \frac{-\Delta t}{t} + \frac{\Delta d}{d} \tag{A-2}$$

Taking the root mean square of the terms in Eqn. A-2, we have

$$\frac{\Delta V_{F,rms}}{V_F} = \left[\left(\frac{\Delta t}{t}\right)^2 + \left(\frac{\Delta d}{d}\right)^2\right]^{1/2} \tag{A-3}$$

where $\Delta V_{F,rms}$ is the probable error in V_F.

The variation of t and d are discussed individually as follows:

$\frac{\Delta t}{t}$: The possible error in time measurement can arise from the following sources

(1) The error in measuring the time. In hand timing the spread rate,

a reflex time of $\pm$ 0.1 s is assumed for each start or stop of the digital clock. The same amount of error is assumed for the response of the microswitches used. The error is not more than 3%.

(2) Uncertainty in reading clocks is less than 0.5%.

(3) The error in the clocks is not more than 1%.

$\frac{\Delta d}{d}$: This error can only be caused by improper reading of the rules and by the error of the rulers themselves. As with the clocks, this is no more than $[1^2 + (0.5)^2]^{1/2}\% = 1.1\%$.

From the above analysis, it is concluded that the probable error for determining V_F, as expressed by equation A-3, is

$$\frac{\Delta V_{F,rms}}{V_F} = [3^2 + (0.5)^2 + 1^2 + (1.1)^2]^{1/2}\% = 3.4\% \quad (A-4)$$

With the present correlation scheme, in which $\bar{\rho}_s \bar{V}_F \bar{\tau}$ depends on $\bar{B}$, errors of $\bar{\rho}_s \bar{V}_F \bar{\tau}$ and $\bar{B}$ should also be discussed. In these two dimensionless parameters, errors in parameters that have been taken as constant are assumed to be zero. These parameters are the gas phase thermal conductivity, k, the gas phase dynamic viscosity, μ, the gas phase specific heat at constant pressure, C_p, the gas phase pre-exponential factor, B, the coefficient of expansion, β, and the characteristic temperature difference, ΔT.

The expression for the dimensionless group $\bar{\rho}_s \bar{V}_F \bar{\tau}$ is repeated here

for convenience.

$$\overline{\rho_s V_F \tau} = \frac{\rho_s V_F \tau}{\mu} \qquad \text{(A-5)}$$

Similar to the error analysis for V_F, the error of $\overline{\rho_s V_F \tau}$ can be written as

$$\frac{\Delta\overline{\rho_s V_F \tau}}{\overline{\rho_s V_F \tau}} = \frac{\Delta\rho_s \tau}{\rho_s \tau} + \frac{\Delta V_F}{V_F} - \frac{\Delta\mu}{\mu} \qquad \text{(A-6)}$$

Under careful calculation of properties used, it is reasonable to assume that the error in the solid phase area density, $\rho_s\tau$, is no more than 4%. Thus, the probable error of $\overline{\rho_s V_F \tau}$, denoted by $\overline{\rho_s V_F \tau}_{rms} \Big/ \overline{\rho_s V_F \tau}$, can be determined as follows

$$\frac{\overline{\rho_s V_F \tau}_{rms}}{\overline{\rho_s V_F \tau}} = \left[\left(\frac{\Delta\rho_s \tau}{\rho_s \tau}\right)^2 + \left(\frac{V_F}{V_F}\right)^2\right]^{1/2}$$

$$= (4^2 + 3.4^2)^{1/2}\% = 5.25\% \qquad \text{(A-7)}$$

The above value represents the maximum probable error of the ordinate in the present correlation.

The Damköhler number, $\overline{B}$, as defined in Eqn. 3.2 is $Bk/(C_p{}^M{}_{ox}(\nu g\beta\Delta T)^{2/3})$. As in the analysis above, the probable error of $\overline{B}$ can be determined by the following equation

$$\frac{\Delta\bar{B}_{rms}}{\bar{B}} = \left[\left(\frac{2}{3}\frac{\Delta P}{P}\right)^2 + \left(\frac{2}{3}\frac{\Delta g}{g}\right)^2\right]^{1/2} \qquad \text{(A-8)}$$

The environment pressure, P, is known to within 1%. The output of the digital voltmeter used to determine the gravity level under which the experiments were conducted showed an oscillation in gravity level due to an imperfection in regulating the rotational speed of the centrifuge. The deviation in gravity level, g, was found to be less than 1.5%. Therefore, the maximum probable error of $\bar{B}$, the abscissa of the dimensionless correlation developed here, is

$$\frac{\Delta\bar{B}_{rms}}{\bar{B}} = \left[\left(\frac{2}{3}\cdot 1\right)^2 + \left(\frac{2}{3}\cdot 1.5\right)^2\right]^{1/2}\% = 1.2\% \qquad \text{(A-9)}$$

APPENDIX B

Effect of Coriolis Acceleration on Flame Spread Rates

A Coriolis acceleration, $2\omega \times \dot{r}$, is always present for an object moving with a radial velocity $\dot{r}$ in a system rotating at an angular speed ω. In all elevated gravity experiments described here, the test chamber was locked at an angle so that the resultant of the centrifugal acceleration and earth normal acceleration was in the same direction as the flame spread. Therefore, gas particles of the buoyant flow induced by the flame downstream of flame attachment have radial velocities, and thus experience a Coriolis acceleration.

For the data reported here, the paper sample orientation was such that the Coriolis acceleration was normal to the sample surface. The magnitude of the Coriolis acceleration is estimated at $2\omega(\nu g\beta\Delta T)^{1/3}$, which after introducing the relationship $g = [\omega^4 R^2 + g_e^2]^{1/2}$ to eliminate ω, becomes $2[(g^2 - g_e^2)/R^2]^{1/4}(\nu g\beta\Delta T)^{1/3}$. At a radius of 6.1 m, the radius used to obtain the data shown in Figs. 12 through 14, the ratio of this acceleration to the acceleration of gravity along the sample surface is 0.06 for the worst case (i.e. at 4g and 20.68 kPa).

The effect of Coriolis acceleration on the results reported here was tested by varying the radius of rotation at constant gravity level. Figure B1 shows that, in general, the spread V_F is independent of Coriolis acceleration.

A Coriolis acceleration tangent to the sample surface can be ob-

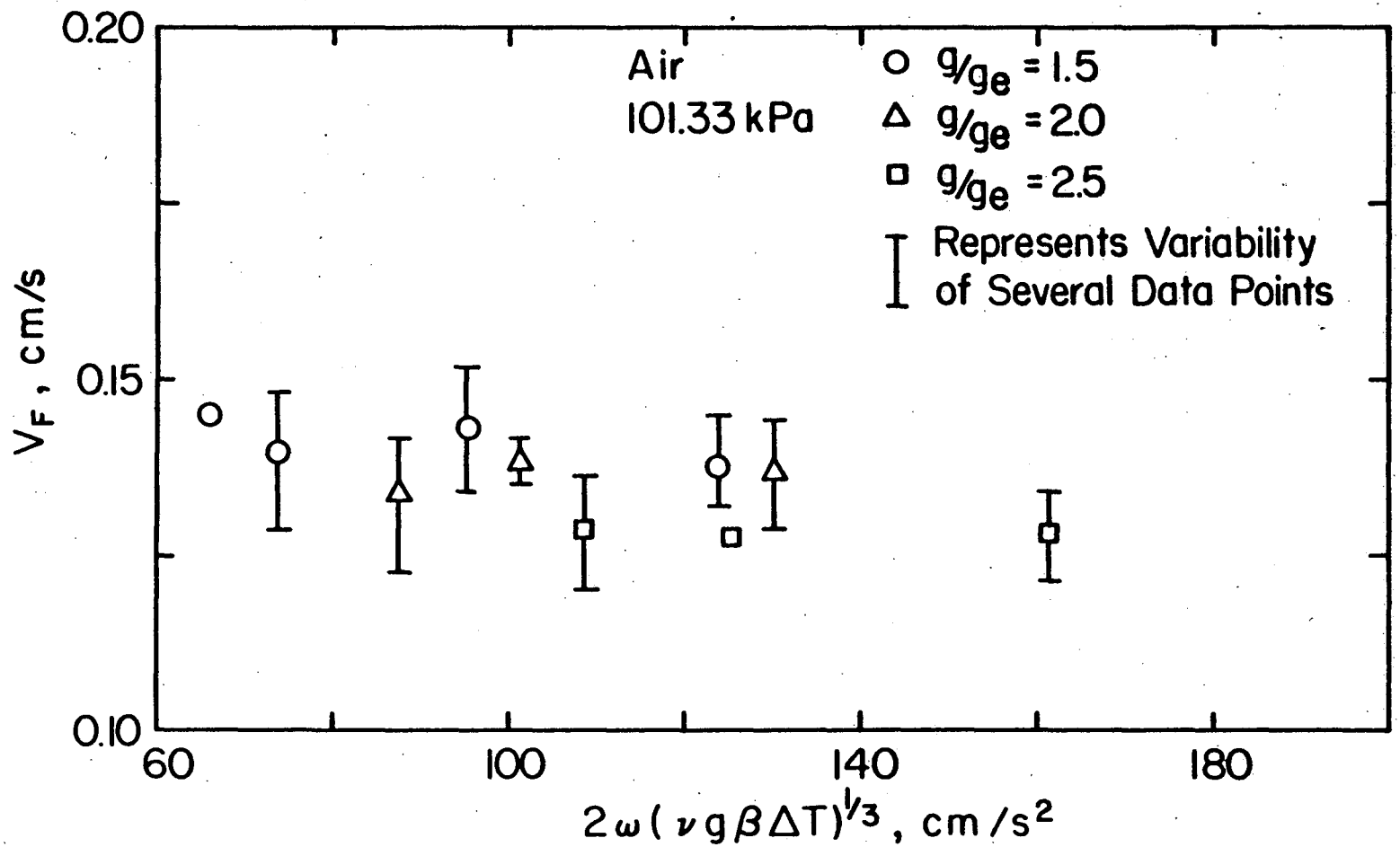

Figure B1 Dependence of V_F on the Coriolis acceleration (index cards)

tained by rotating the chamber by 90 degrees about its axis of symmetry. Spread rate results (Appendix C) obtained with this configuration show a different extinction limit. The flame extinguishes at higher values of the Damköhler number when the Coriolis acceleration vector is tangent, rather than normal, to the sample surface. Apparently, a cross flow, due to the tangential acceleration, blows the flame out prematurely.

APPENDIX C

TABULATION AND REDUCTION OF DATA

1. Data Used in Correlations

All gas phase physical properties were evaluated at 1500 K. $\beta\Delta T$ was set equal to 4. Values of the dynamic viscosity, μ, the specific heat, C_p, and the thermal conductivity, k, of air were obtained from Ref. [24]. Values of these physical properties for pure oxygen and pure nitrogen were obtained from Refs. [25] and [26]. The 50% O_2/ 50% N_2 mixture's dynamic viscosity and the thermal conductivity were calculated by equations 9-5.4 and 10-6.9 of Ref. [27]. Molecular weights of air and 50% O_2/50% N_2 mixture are 28.97 g/mol and 30 g/mol, respectively. The ideal gas law was used throughout to calculate the gas phase density.

The property values used are listed below:

Air at 1500 K and atmospheric pressure:

$$C_p = 1.230 \times 10^3 \text{ J/(kg•K)}$$

$$k = 0.0946 \text{ J/(s•m•K)}$$

$$\mu = 5.40 \times 10^{-5} \text{ kg/(m•s)}$$

50% O_2/50% N_2 mixture at 1500 K and atmospheric pressure:

$$C_p = 1.194 \times 10^3 \text{ J/(kg•K)}$$

$$k = 0.0931 \text{ J/(s•m•K)}$$

$$\mu = 5.63 \times 10^{-5} \text{ kg/(m•s)}$$

The area density, $\rho_s \tau$, of the paper tape and index cards was measured to be $2.890 \times 10^{-3} g/cm^2$ and $7.381 \times 10^{-3} g/cm^2$, and the respective half thicknesses are 0.0043 cm and 0.0098 cm. The pre-exponential factor, $B = 1 \times 10^{12} cm^3/(mol \cdot s)$, was taken from Ref. [19].

The vertical downward flame spread data have been arranged in order of increasing pressure for each gas mixture and sample thickness. Each data point listed represents an average of several spread measurements. An asterisk (*) indicates that one or more attempts yielded flames which could not propagate.

Pressure (kPa)	g/g_e	V_F (cm/s)	$\overline{B}$ ($\times 10^4$)	$\overline{\rho}_s \overline{V}_F \overline{\tau}$
		Air; Index Cards		
68.93	1.00	0.147	4.301	2.007
	1.50	0.134	3.282	1.829
	1.75	0.129	2.962	1.761
	2.00	0.117	2.709	1.597
	2.50	0.116*	2.335	1.584*
	3.00	*	2.068	*
86.16	1.00	0.157	4.991	2.143
	1.50	0.145	3.809	1.980
	2.00	0.136	3.144	1.857
	2.50	0.126*	2.709	1.720*
	3.00	0.123*	2.399	1.679*
	3.50	*	2.165	*
101.33	1.00	0.154	5.560	2.102
	1.50	0.145	4.243	1.980
	1.75	0.142	3.829	1.939
	2.00	0.134	3.503	1.829
	3.25	0.122	2.534	1.666
	3.50	0.115*	2.412	1.570*
	4.00	0.112*	2.207	1.529*
	4.25	*	2.119	*
137.86	1.00	0.157	6.827	2.143
	2.00	0.146	4.301	1.993
	3.00	0.137	3.282	1.870
	4.00	0.117	2.709	1.597
275.72	1.00	0.177	10.840	2.416
	2.00	0.157	6.287	2.143
	3.00	0.145	5.210	1.980
	4.00	0.140	4.301	1.911

413.58	1.00	0.178	14.200	2.430
	2.00	0.161	8.946	2.198
	3.00	0.154	6.827	2.102
	3.50	0.151	6.160	2.061
	4.00	0.145	5.636	1.980
Air; Paper Tape				
68.93	1.00	0.369	4.301	1.985
	3.00	0.283	2.068	1.522
	3.50	0.280*	1.866	1.506*
	4.00	*	1.707	*
101.33	1.00	0.396	5.560	2.130
	1.50	0.358	4.243	1.926
	2.00	0.363	3.503	1.953
	2.50	0.324	3.019	1.743
	3.00	0.307	2.673	1.651
	3.50	0.298	2.412	1.603
	4.00	0.285	2.207	1.533
137.86	1.00	0.403	6.827	2.168
275.72	1.00	0.419	10.840	2.254
413.58	1.00	0.422	14.200	2.270
50% O_2/50% N_2; Index Cards				
28.68	1.00	0.525	1.943	6.995
	1.50	0.499	1.483	6.649
	2.00	0.469	1.224	6.249
	2.50	0.460	1.055	6.129
	3.00	0.447	0.934	5.956
	3.50	0.424	0.843	5.650
	4.00	0.468	0.771	6.236
34.47	1.00	0.550	2.732	7.328
	1.50	0.519	2.085	6.995
	2.00	0.519	1.721	6.915

	2.50	0.512	1.483	6.822
	3.00	0.512	1.314	6.822
	3.50	0.492	1.185	6.549
	4.00	0.493	1.084	6.569
68.93	1.00	0.569	4.337	7.582
	2.00	0.540	2.732	7.160
	3.00	0.554	2.085	7.345
	4.00	0.553	1.721	7.332
101.33	1.00	0.602	5.607	7.982
	2.00	0.600	3.532	7.955
	2.50	0.566	3.044	7.542
	3.00	0.547	2.696	7.284
	4.00	0.539	2.225	7.177
275.72	1.00	0.617	10.930	8.214
551.58	1.00	0.646	17.350	8.601

50% O_2/50% N_2; Paper Tape

20.68	3.00	1.221	0.934	6.495
34.47	1.00	1.355	2.732	7.207
	3.00	1.298	1.313	6.904
68.93	1.00	1.430	4.337	7.606
	3.00	1.324	2.085	7.042
101.33	1.00	1.498	5.607	7.967
275.72	1.00	1.502	10.920	7.987
551.58	1.00	1.475	17.350	7.846

2. Elevated Gravity Data With Tangential Coriolis Acceleration

The elevated gravity data for vertical downward flame spread with Coriolis acceleration tangent to the specimen surface are listed below in the order of increasing pressure. Values used for various parameters are the same as those used in reducing the data that appear in the previous section. Again, these data are the average of several runs and asterisks indicate that one or more attempts to obtain steadily propagating flames failed.

Pressure	a/g_e	V_F (cm/s)	$\overline{B}$ (x 10^4)	$\overline{\rho_s}\ \overline{V_F}\ \overline{\tau}$
		Air; Index Cards		
68.93	1.50	*	3.282	*
86.16	1.50	0.131	3.809	1.788
	1.75	0.127	3.437	1.734
	2.00	0.121	3.144	1.652
101.33	1.50	0.145	4.243	1.980
	1.75	0.141	3.829	1.925
	2.00	0.129	3.503	1.761
	2.50	0.126	3.019	1.720
	3.00	0.113	2.673	1.543
	3.25	*	2.534	*